

Searches for Supersymmetry at High-Energy Colliders

Jonathan L. Feng,¹ Jean-François Grivaz,² and Jane Nachtman³

¹*Department of Physics and Astronomy, University of California, Irvine, CA 92697, USA*

²*Laboratoire de l'Accélérateur Linéaire, Orsay, France*

³*University of Iowa, Iowa City, Iowa 52242, USA*

This review summarizes the state of the art in searches for supersymmetry at colliders on the eve of the LHC era. Supersymmetry is unique among extensions of the standard model in being motivated by naturalness, dark matter, and force unification, both with and without gravity. At the same time, weak-scale supersymmetry encompasses a wide range of experimental signals that are also found in many other frameworks. We recall the motivations for supersymmetry and review the various models and their distinctive features. We then comprehensively summarize searches for neutral and charged Higgs bosons and standard model superpartners at the high energy frontier, considering both canonical and non-canonical supersymmetric models, and including results from LEP, HERA, and the Tevatron.

PACS numbers: 12.60.Jv, 13.85.Rm, 14.80.Cp, 14.80.Ly

Contents

I. Introduction	1
A. Motivations for New Phenomena	1
1. Naturalness	1
2. Dark Matter	2
3. Unification	2
B. Experimental context	2
II. Supersymmetric Models and Particles	3
A. Superpartners	4
B. Supersymmetry Parameters	5
C. Unifying Frameworks	5
1. Gravity Mediation (SUGRA)	6
2. GMSB	6
3. AMSB	7
D. Supersymmetric Higgs Bosons	7
E. Neutralinos and Charginos	8
F. Sleptons	8
G. Squarks	8
III. Searches for MSSM neutral Higgs bosons	8
A. MSSM benchmark scenarios	8
B. Searches at LEP	9
C. Searches at the Tevatron	11
IV. Searches for charged Higgs bosons	12
A. Searches at LEP	13
B. Searches at the Tevatron	13
V. Searches for supersymmetric particles	15
A. General features of SUSY models	15
B. Signatures and strategies	16
C. Searches in the canonical scenario	17
1. Searches at LEP	17
2. Searches at the Tevatron	19
D. Searches in non-canonical scenarios	22
1. R -parity violation	22
2. Gauge-mediated SUSY breaking	22
3. Other non-canonical scenarios	23
VI. Summary	24
References	25

I. INTRODUCTION

Particle physics is at a crossroads. Behind us is the standard model (SM), the remarkably successful theory of all known elementary particles and their interactions. Ahead of us is an equally remarkable array of possibilities for new phenomena at the weak scale. Never before has an energy scale been so widely anticipated to yield profound insights, and never before have there been so many ideas about exactly what these insights could be. In this article, we review the current state of experimental searches for supersymmetry, the most widely studied extension of the SM.

A. Motivations for New Phenomena

There are at present many reasons to expect new physics at the weak scale $m_{\text{weak}} \sim 100 \text{ GeV} - 1 \text{ TeV}$. Chief among these is the Higgs boson, an essential component of the SM that has yet to be discovered. At the same time, there are also strong motivations for new phenomena beyond the Higgs boson. These motivations include naturalness, dark matter, and unification.

1. Naturalness

The physical mass of the SM Higgs boson is given by

$$m_h^2 = m_h^{0,2} + \Delta m_h^2, \quad (1)$$

where $m_h^{0,2}$ is the bare mass parameter present in the Lagrangian, and the quantum corrections are

$$\Delta m_h^2 \sim \frac{\lambda^2}{16\pi^2} \int^\Lambda \frac{d^4p}{p^2} \sim \frac{\lambda^2}{16\pi^2} \Lambda^2, \quad (2)$$

where λ is a dimensionless gauge or Yukawa coupling, and Λ is the energy scale at which the SM is no longer

a valid description of nature. Because Δm_h^2 is proportional to Λ^2 (“quadratically divergent”), it is natural to expect the Higgs mass to be pulled up to within an order of magnitude of Λ by quantum corrections (1; 2; 3; 4). Given that unitarity and precision constraints require m_h to be at the weak scale, this implies $\Lambda \lesssim 1$ TeV, and new physics should appear at the current energy frontier. Of course, the Higgs boson may not be a fundamental scalar, but in this case, too, its structure requires new physics at the weak scale. For these reasons, naturalness is among the most robust motivations for new physics at an energy scale accessible to accelerator-based experiments.

2. Dark Matter

In the last decade, a wealth of cosmological observations have constrained the energy densities of baryons, non-baryonic dark matter, and dark energy, in units of the critical density, to be (5)

$$\begin{aligned}\Omega_B &= 0.0462 \pm 0.0015 \\ \Omega_{\text{DM}} &= 0.233 \pm 0.013 \\ \Omega_\Lambda &= 0.721 \pm 0.015 .\end{aligned}\tag{3}$$

The non-baryonic dark matter must be stable or very long-lived and dominantly cold or warm. None of the particles of the SM satisfies these conditions, and so cosmology requires new particles.

Perhaps the simplest production mechanism for dark matter is thermal freeze out (6; 7; 8; 9). In this scenario, a new particle is initially in thermal contact with the SM, but as the Universe cools and expands, this particle loses thermal contact and its energy density approaches a constant. Under very general assumptions, this relic energy density satisfies

$$\Omega_X \propto \frac{1}{\langle \sigma v \rangle} ,\tag{4}$$

where $\langle \sigma v \rangle$ is the dark matter’s thermally-averaged annihilation cross section. It is a tantalizing fact that, when this cross section is typical of weak-scale particles, that is, $\sigma v \sim \alpha^2/m_{\text{weak}}^2$, where $m_{\text{weak}} \sim 100$ GeV, Ω_X is near the observed value of Ω_{DM} given in Eq. (3). If thermal freeze out is the mechanism by which dark matter is produced in the early Universe, then, cosmological data therefore also point to the weak scale as the natural scale for new physics.

3. Unification

The SM is consistent with the observed properties of all known elementary particles. It also elegantly explains why some phenomena, such as proton decay and large flavor-changing neutral currents, are not observed. The latter fact is highly non-trivial, as evidenced by the intellectual contortions required of model builders who try to extend the SM.

At the same time, the SM contains many free parameters with values constrained by experiment, but not explained. The number of free parameters may be reduced in unified theories, in which the symmetries of the SM are extended to larger symmetries. In particular, grand unified theories, in which the $SU(3) \times SU(2) \times U(1)$ gauge structure is extended to larger groups, are significantly motivated by the fact that the SM particle content fits perfectly into multiplets of $SU(5)$ and larger groups (10), potentially explaining the seemingly random assignment of quantum numbers, such as hypercharge.

One straightforward implication of the simplest ideas of grand unification is that the gauge couplings of the SM must unify when extrapolated to higher scales through renormalization group evolution. The gauge couplings do not unify at any scale given the particle content of the SM, but they do unify at the value $g_U \simeq 0.7$ at $M_{\text{GUT}} \simeq 2 \times 10^{16}$ GeV if the SM is minimally extended by supersymmetry (SUSY) and the supersymmetric particles are at the weak scale (11; 12; 13; 14; 15). This unification is highly non-trivial, not only because the couplings are now so precisely measured, but also because g_U is in the perturbative regime and M_{GUT} is in the narrow range that is both high enough to suppress proton decay and low enough to avoid quantum gravitational effects. This unification is only logarithmically sensitive to the superpartner mass scale, and the degree of its success is somewhat model-dependent. In conjunction with the previous two motivations, however, it provides still more evidence for new physics at the weak scale, and selects supersymmetry as a particularly motivated possibility.

B. Experimental context

There are two main areas where new phenomena could appear in particle physics. Deviations from SM predictions could show up in measurements performed with increasing precision. Examples are the anomalies observed in the forward-backward asymmetry in the production of $b\bar{b}$ pairs in e^+e^- collisions at the Z peak, or in the anomalous magnetic moment of the muon. Even if such anomalies receive experimental confirmation at a sufficient significance level, their interpretation will however remain ambiguous, because it will involve virtual contributions to the relevant amplitudes of yet undiscovered, therefore most likely very massive, particles. The alternative approach is to try to observe directly the production of these new particles, which is among the goals of the experiments at colliders operating at the highest possible energies.

The Large Hadron Collider (LHC) at CERN will soon occupy the energy frontier. When it comes into operation, pp collisions will take place at a center-of-mass energy of 10 TeV, and of 14 TeV later on. The instantaneous luminosity will be raised first to 10^{32} $\text{cm}^{-2} \text{s}^{-1}$ and progressively to 10^{34} $\text{cm}^{-2} \text{s}^{-1}$. With the enormous data samples accumulated, the two general purpose ex-

periments at the LHC, ATLAS (16) and CMS (17), will be in a position to explore in great detail the physics at the TeV scale. Since this is an entirely new domain, and since there are strong reasons to expect new phenomena at that scale, as advocated in the preceding section of this review, it may well be that ground breaking discoveries are made at the LHC, even after a short period of operation, once the detectors are properly aligned, calibrated, and well understood.

Until then, the most constraining results on searches for new phenomena at high energy have been or are still being obtained at LEP, HERA, and the Tevatron. Providing a comprehensive account of such searches for supersymmetry is the purpose of this review.

The large e^+e^- collider (LEP) at CERN operated from 1989 to 2000. In a first phase (LEP1), the center-of-mass energy was set at or close to 91 GeV, the peak of the Z boson resonance. Four experiments, ALEPH (18), DELPHI (19), L3 (20), and OPAL (21) collected millions of Z decays that allowed them to perform stringent precision tests of the SM. From the end of 1995 on, the energy was progressively increased (LEP2) to reach 209 GeV in the center of mass during the last year of operation. Altogether, each of the experiments collected a total of $\sim 1 \text{ fb}^{-1}$ of data, of which $\sim 235 \text{ pb}^{-1}$ was collected in 2000 at and above 204 GeV, the data set most relevant for new particle searches.

At DESY, the HERA collider operation was terminated in June 2007. There, $e^\pm p$ collisions were collected by two experiments, H1 (22) and ZEUS (23), at a center-of-mass energy of $\sim 300 \text{ GeV}$. This was an asymmetric collider, with e^\pm and proton beam energies of 30 and 820 GeV, respectively. An upgrade took place in 2001 (HERA2), leading to higher luminosities than in the previous phase (HERA1), and allowing operation with polarized e^\pm beams. The data sets collected at HERA1 and HERA2 with electron or positron beams altogether correspond to an integrated luminosity of $\sim 0.5 \text{ fb}^{-1}$ per experiment.

Until the LHC comes into operation, the highest energy collisions are provided by the Tevatron at Fermilab. Two phases are distinguished for the operation of this $p\bar{p}$ collider. During the first one (Run I), the center-of-mass energy was set to 1.8 TeV, and $\sim 110 \text{ pb}^{-1}$ were collected by each of the two experiments, CDF (24) and DØ (25). The highlight of that period was the discovery of the top quark in 1995. Major upgrades of the accelerator complex and of the two detectors took place for the second phase (Run II), which began in 2001. The center-of-mass energy was raised to 1.96 TeV, and the instantaneous luminosity was progressively increased to regularly approach or exceed $3 \times 10^{32} \text{ cm}^{-2} \text{ s}^{-1}$ in 2008. More than 5 fb^{-1} had been delivered by the Tevatron by the end of fiscal year (FY) 2008, and it is expected that another $\sim 1.5 \text{ fb}^{-1}$ will be provided per additional year of operation. At the time of writing, running in FY 2009 is underway, running in FY 2010 is increasingly likely, and running in FY 2011 is kept as an option.

All general purpose detectors at colliders share similar features. A cylindrical “barrel” structure parallel to the beam axis surrounds the interaction region, and is closed by “end caps” perpendicular to the beam. The first elements encountered beyond the beam pipe are charged-particle detectors, with those closest to the interaction point benefiting from the highest spatial precision. This tracking system is immersed in an axial magnetic field provided by a solenoidal magnet. Beyond the tracking system, electromagnetic calorimeters provide electron and photon identification and energy measurement. These are followed by hadron calorimeters for the measurement of jet energies. Finally, track detectors are used to identify and measure the muons which have penetrated through the calorimeters and possibly additional absorber material.

Non-interacting particles, such as neutrinos, are detected by an apparent non-conservation of energy and momentum. In e^+e^- annihilation, the missing energy and momentum can be directly inferred from a measurement of the final state particles, by comparison with the center-of-mass energy of the collision. In hadronic or ep collisions, the partons participating in the hard process carry only a fraction of the beam energy, and the beam remnants associated with the spectator partons largely escape undetected in the beam pipe. As a consequence, only conservation of the momentum in the direction transverse to the beams can be used, and the relevant quantity is the missing transverse energy \cancel{E}_T , rather than the total missing energy.

The mass reach in $p\bar{p}$ collisions at the Tevatron is expected to be substantially larger than at LEP because of the higher center-of-mass energy. However, since the initial partons participating in the hard process carry fractions x_1 and x_2 of the beam energy, the effective center-of-mass energy is only $\sqrt{\hat{s}} = \sqrt{x_1 x_2 s}$. Because of the rapidly falling parton distribution functions (PDFs) as a function of those energy fractions, increasingly large integrated luminosities are needed to probe larger and larger $\sqrt{\hat{s}}$ values. At HERA, furthermore, the center-of-mass energy in the eq collision cannot be fully used for new particle production, except in some very specific instances. This is in contrast to e^+e^- or $q\bar{q}$ annihilation, and to gg fusion. As a consequence, the most constraining results on new particle searches typically come from LEP and from the Tevatron.

In the following, all limits quoted are given at a confidence level of 95%.

II. SUPERSYMMETRIC MODELS AND PARTICLES

Supersymmetry (SUSY) (26; 27; 28) is an extension of Poincare symmetry, which encompasses the known space-time symmetries of translations, rotations, and boosts. As with the Poincare and internal symmetries, SUSY transforms particle states to other particle states. In contrast to these other symmetries, however, SUSY relates

states of different spin, transforming fermions into bosons and vice versa. None of the known particles can be supersymmetric partners of other known particles. As a result, SUSY predicts many new particle states. If SUSY were exact, these particles would be degenerate with known particles. Since this is experimentally excluded, if SUSY is a symmetry of nature, it must be broken.

SUSY is the most studied extension of the SM because it directly addresses several of the motivations for new physics discussed in Sec. I. In supersymmetric theories, the quadratically divergent loop contributions to the Higgs boson mass from SM particles are canceled by similar contributions from superpartners, ameliorating the gauge hierarchy problem (29; 30; 31). Supersymmetric theories also include excellent dark matter candidates, in the form of neutralinos (32; 33) and gravitinos (34; 35), that may naturally have the desired relic density. Finally, SUSY is strongly motivated by the hope for unifying forces, as it makes gauge coupling unification possible in simple grand unified theories (GUTs) (11; 12; 13; 14; 15). It is important to note that *all* of these virtues are preserved only if the superpartner mass scale is around the weak scale. The existence of SUSY in nature, although not necessarily at the weak scale, is also motivated by string theory and the beautiful mathematical properties of SUSY that are beyond the scope of this review.

For these reasons, this review is devoted to searches for SUSY at colliders. In this Section, we present brief summaries of the supersymmetric spectrum, parameters, and unifying frameworks to establish our conventions and notation.

A. Superpartners

In this review, we focus our attention on the minimal supersymmetric extension of the standard model (MSSM), the supersymmetric model with minimal field content. Bosonic superpartners are given names with the prefix “s-,” and fermionic superpartners are denoted by the suffix “-ino.” Squarks and sleptons are collectively known as “sfermions,” and the entire group of superpartner particles are often called “sparticles.”

The particle content of the MSSM is in fact slightly more than a doubling of the SM particle content. This is because, in addition to introducing superpartners for all known particles, the MSSM requires two electroweak Higgs doublets. There are two reasons for this. First, in the SM, mass terms are generated for up- and down-type particles by Yukawa couplings to φ^* and φ , respectively, where φ is the SM Higgs field. In SUSY, Yukawa couplings are generalized to terms in a superpotential, which generates the SM Yukawa couplings as well as all other terms related to these by SUSY. Complex-conjugated fields are not allowed in the superpotential, however. As a result, two separate Higgs fields, denoted H_u and H_d , are required to generate masses through the superpoten-

tial terms

$$W = \lambda_u H_u Q \bar{U} + \lambda_d H_d Q \bar{D} + \lambda_e H_d L \bar{E}, \quad (5)$$

where Q , U , D , L , and E are the SU(2) quark doublet, up-type quark singlet, down-type quark singlet, lepton doublet, and lepton singlet, respectively, and the λ couplings are Yukawa couplings. Second, SUSY requires that the SM Higgs field have fermion partners, the Higgsinos. The introduction of these additional fermions charged under SM gauge groups ruins anomaly cancellation, making this theory mathematically untenable. The introduction of an additional Higgs doublet, with its extra Higgsinos, restores anomaly cancellation.

The MSSM Higgs boson sector therefore consists of eight degrees of freedom. As in the SM, three of these are eaten to make massive W and Z bosons, but five remain, which form 4 physical particles:

$$\text{MSSM Higgs Bosons (Spin 0)} : \quad h, H, A, H^\pm, \quad (6)$$

where h and H are the CP-even neutral Higgs bosons, with h lighter than H , A is the CP-odd neutral Higgs boson, and H^\pm is the charged Higgs boson.

The remaining supersymmetric particle content of the MSSM is straightforward to determine and consists of the following states:

$$\begin{aligned} \text{Neutralinos (Spin 1/2)} : & \quad \tilde{B}, \tilde{W}^0, \tilde{H}_u^0, \tilde{H}_d^0 \\ \text{Charginos (Spin 1/2)} : & \quad \tilde{W}^+, \tilde{H}_u^+ \\ & \quad \tilde{W}^-, \tilde{H}_d^- \\ \text{Sleptons (Spin 0)} : & \quad \tilde{e}_{L,R}, \tilde{\mu}_{L,R}, \tilde{\tau}_{L,R} \\ & \quad \tilde{\nu}_e, \tilde{\nu}_\mu, \tilde{\nu}_\tau \\ \text{Squarks (Spin 0)} : & \quad \tilde{u}_{L,R}, \tilde{c}_{L,R}, \tilde{t}_{L,R} \\ & \quad \tilde{d}_{L,R}, \tilde{s}_{L,R}, \tilde{b}_{L,R} \\ \text{Gluinos (Spin 1/2)} : & \quad \tilde{g}. \end{aligned} \quad (7)$$

Each SM chiral fermion has a (complex) scalar partner, denoted by the appropriate chirality subscript. The dimensionless couplings of all of these particles are fixed by SUSY to be identical to those of their SM partners. Note, however, that, as described in the appropriate sections below, the states in each line of Eq. (7) (except for the last one) may mix, and mass eigenstates are in general linear combinations of these gauge eigenstates.

Finally, most analyses of SUSY include the supersymmetric partner of the graviton:

$$\text{Gravitino (Spin 3/2)} : \quad \tilde{G}. \quad (8)$$

Although not technically required as a part of the MSSM, when SUSY is promoted to a local symmetry, it necessarily includes gravity, and the resulting supergravity theories include both gravitons and gravitinos. The gravitino is therefore present if SUSY plays a role in unifying the SM with gravity, as in string theory.

If SUSY were exact, the gravitino’s properties would be determined precisely by the graviton’s, and it would be

massless and have gravitational couplings suppressed by the reduced Planck mass $M_* \simeq 2.4 \times 10^{18}$ GeV. However, just as Goldstone bosons appear when conventional symmetries are spontaneously broken, a fermion, the Goldstino $\tilde{G}_{1/2}$, appears when SUSY is broken. The gravitino then becomes massive by eating the Goldstino. In terms of F , the mass dimension-2 order parameter of SUSY breaking, the gravitino mass becomes

$$m_{\tilde{G}} \sim \frac{F}{M_*}, \quad (9)$$

and, very roughly, its interactions in processes probing energy scale E may be characterized by a dimensionless coupling

$$g_{\tilde{G}} \sim \frac{E^2}{F} \sim \frac{E^2}{m_{\tilde{G}} M_*}. \quad (10)$$

Light gravitinos couple more strongly. As we will see below, in well-motivated supersymmetric theories, these properties may take values in the range

$$\text{eV} \lesssim m_{\tilde{G}} \lesssim 10 \text{ TeV} \quad (11)$$

$$10^{-5} \gtrsim g_{\tilde{G}} \gtrsim 10^{-18}, \quad (12)$$

where we have assumed colliders probing $E \sim m_{\text{weak}}$.

B. Supersymmetry Parameters

As noted above, if SUSY exists in nature, it must be broken. Although many different Lagrangian terms could be added to break SUSY, only some of these are allowed if SUSY is to stabilize the gauge hierarchy. These terms, known as “soft” SUSY-breaking terms, include most, but not all, Lagrangian terms with mass dimension 3 and below (36). For the MSSM, they are

$$\begin{aligned} & m_{\tilde{Q}}^2 |\tilde{Q}|^2 + m_{\tilde{U}}^2 |\tilde{U}|^2 + m_{\tilde{D}}^2 |\tilde{D}|^2 + m_{\tilde{L}}^2 |\tilde{L}|^2 + m_{\tilde{E}}^2 |\tilde{E}|^2 \\ & + \frac{1}{2} \left\{ \left[M_1 \tilde{B} \tilde{B} + M_2 \tilde{W}^j \tilde{W}^j + M_3 \tilde{g}^k \tilde{g}^k \right] + \text{h.c.} \right\} \\ & + \lambda_u A_U H_u \tilde{Q} \tilde{U} + \lambda_d A_D H_d \tilde{Q} \tilde{D} + \lambda_e A_E H_d \tilde{L} \tilde{E} \\ & + m_{H_u}^2 H_u^* H_u + m_{H_d}^2 H_d^* H_d + (B H_u H_d + \text{h.c.}). \end{aligned} \quad (13)$$

These lines are sfermion masses, gaugino masses, trilinear scalar couplings (“ A -terms”), and Higgs boson couplings. In addition to the parameters above, there are two other key parameters: the μ parameter, which enters in the Higgsino mass terms $\mu \tilde{H}_u^i \tilde{H}_d^i$, and

$$\tan \beta \equiv \frac{\langle H_u^0 \rangle}{\langle H_d^0 \rangle}, \quad (14)$$

which parameterizes how the SM Higgs vacuum expectation value is divided between the two neutral Higgs scalars.

The interactions of Eq. (13) conserve R -parity (37; 38). With $R = (-1)^{3(B-L)+2S}$, where B and L are the baryon

and lepton numbers, respectively, and S the spin, all superpartners are odd and all SM particles are even under R -parity. This implies that all interactions involve an even number of superpartners, and so the lightest superpartner is stable, and a potential dark matter candidate. R -parity violation generically violates both baryon and lepton number, leading to too-rapid proton decay, which is why, for most of this review, we limit ourselves to the R -parity conserving case.

Even restricting ourselves to the R -parity-preserving terms of Eq. (13), however, we see that SUSY introduces many new parameters. Note that the terms involving sfermions need not be flavor-diagonal, and so the sfermion masses and A -terms are in fact matrices of parameters in the most general case. At the same time, fully general flavor mixing terms violate low energy constraints on flavor-changing neutral currents. In addition, arbitrary complex parameters also violate bounds on CP-violation from, for example, ϵ_K and the electric dipole moments of the electron and neutron. These considerations motivate unifying frameworks, to which we now turn.

C. Unifying Frameworks

In collider searches, it is desirable to consider theories that are both viable and simple enough to be explored fully. For this reason, it is common to work in simple model frameworks that reduce the number of independent SUSY parameters. In some cases, these model frameworks also motivate particular collider signatures that might otherwise appear highly unlikely or fine-tuned.

In the most common unifying frameworks, SUSY is assumed to be broken in some other sector. SUSY breaking is then mediated to the MSSM through a mechanism that defines the framework. This sets SUSY-breaking parameters at some high energy scale. Renormalization group evolution to the weak scale then determines the physical soft SUSY-breaking parameters and the physical spectrum of the MSSM. A representative example of renormalization group evolution is shown in Fig. 1. In this evolution from the high scale to the weak scale, gauge couplings increase masses and Yukawa couplings decrease masses. This is central to understanding the sparticle spectrum of many models. In addition, it explains why $m_{H_u}^2$ becomes negative at the weak scale — it is the only particle to receive large negative contributions from Yukawa couplings without compensating large positive contributions from the strong coupling. When H_u becomes tachyonic, it breaks electroweak symmetry, and this feature, known as “radiative electroweak symmetry breaking,” is a virtue of many supersymmetric frameworks.

In this section, we discuss several common unifying frameworks that have been used in collider searches, namely, models with gravity-, gauge-, and anomaly-

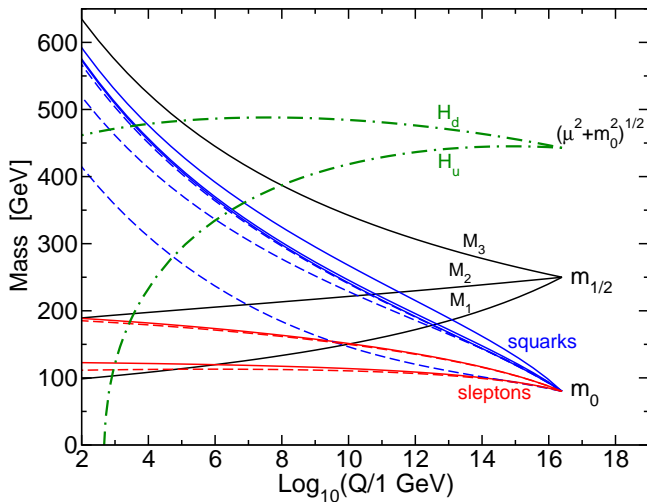


FIG. 1 Renormalization group evolution of scalar and gaugino mass parameters from the GUT scale $M_{\text{GUT}} \simeq 2 \times 10^{16}$ GeV to the weak scale in a representative mSUGRA model. From Ref. (39).

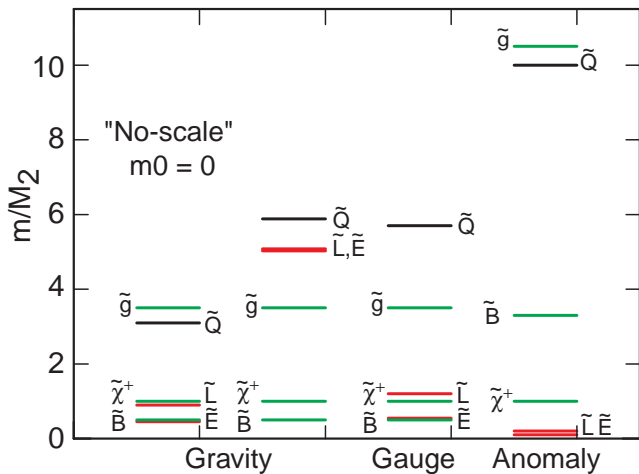


FIG. 2 Sparticle spectra for representative models with gravity-, gauge-, and anomaly-mediated SUSY breaking. The masses are normalized to M_2 , the Wino mass parameter at the weak scale. In the gravity-mediated case, two example spectra are presented: one for “no-scale” models with $m_0 = 0$, and another for $m_0 = 5M_2$. In the anomaly-mediated case, the sleptons are tachyonic in the minimal case — additional effects are required to raise these to a viable range. From Ref. (40).

mediated SUSY breaking. Each of these has its distinctive characteristics. As a rough guide, in Fig. 2 we show representative spectra resulting from each of these frameworks.

1. Gravity Mediation (SUGRA)

In gravity-mediated SUSY-breaking models (41; 42; 43; 44), sometimes referred to as supergravity (SUGRA) models, SUSY breaking in a hidden sector is mediated to the MSSM through terms suppressed by the reduced Planck mass M_* . For example, sfermion masses are $m_{\tilde{f}} \sim F/M_*$. For these to be at the weak scale, \sqrt{F} must be around 10^{11} GeV. Given Eqs. (9) and (10), the gravitino also has a weak scale mass and couples with gravitational strength in SUGRA models.

Without a quantum theory of gravity, the structure of gravity-mediated SUSY parameters is unconstrained and generically violates low-energy constraints. To make these theories viable, *ad hoc* unifying assumptions must be made. By far the most common assumptions are those of minimal supergravity (mSUGRA), which is specified by 4 continuous and 1 discrete parameter choice:

$$\text{mSUGRA: } m_0, m_{1/2}, A_0, \tan \beta, \text{sign}(\mu), \quad (15)$$

where the first three parameters are the universal scalar mass (including the two Higgs scalars), unified gaugino mass, and universal A -parameter, which are all specified at the grand unified theory (GUT) scale $M_{\text{GUT}} \simeq 2 \times 10^{16}$ GeV. The remaining SUSY parameters $|\mu|$ and B are determined by requiring that the Higgs potential at the weak scale give correct electroweak symmetry breaking. At tree-level, this requires

$$\frac{1}{2}m_Z^2 = \frac{m_{H_d}^2 - m_{H_u}^2 \tan^2 \beta}{\tan^2 \beta - 1} - |\mu|^2 \quad (16)$$

$$\sin 2\beta = \frac{2B}{m_{H_d}^2 + m_{H_u}^2 + 2|\mu|^2}. \quad (17)$$

Gaugino mass unification is motivated by the unification of gauge couplings at M_{GUT} in the MSSM. It leads to the prediction $M_1 : M_2 : M_3 \simeq 1 : 2 : 7$ at the weak scale, as evident in Fig. 2. Scalar mass universality is on much less solid ground. Even in GUTs, for example, the Higgs scalars are not necessarily in the same multiplet as the squarks and sleptons. This motivates a slightly less restrictive framework, the non-universal Higgs model (NUHM) in which m_0 is the universal sfermion mass, but m_{H_u} and m_{H_d} are treated as independent parameters. One may exchange these new degrees of freedom for the more phenomenological parameters μ and m_A at the weak scale:

$$\text{NUHM: } m_0, m_{1/2}, A_0, \tan \beta, \mu, m_A, \quad (18)$$

The NUHM framework is employed in some MSSM Higgs boson studies discussed in Sec. II.D.

2. GMSB

In gauge-mediated SUSY-breaking (GMSB) models (45; 46; 47; 48; 49; 50), in addition to the gravity-mediated contributions to soft parameters discussed

above, each sparticle receives contributions to its mass determined by its gauge quantum numbers. These new contributions to sfermion masses are $\sim F/M_{\text{mess}}$, where M_{mess} is the mass scale of the messenger particles that transmit the SUSY breaking. The GMSB contributions are flavor-blind, and do not violate low energy bounds. For these to be dominant, one requires $M_{\text{mess}} \lesssim 10^{14}$ GeV, and so we find that $m_{\tilde{G}} \sim F/M_* \ll F/M_{\text{mess}} \sim m_{\text{weak}}$ in GMSB scenarios, and the lightest supersymmetric particle (LSP) is always the gravitino.

In GMSB models, the collider signatures are determined by the next-to-lightest supersymmetric particle (NLSP) and its lifetime, or equivalently, the gravitino's mass. If the NLSP is the lightest neutralino, the collider signature is either missing energy or prompt photons, Z s or Higgs bosons from $\tilde{\chi}^0 \rightarrow (\gamma, Z, h)\tilde{G}$ (51); if the NLSP is a slepton, the signature is typically either long-lived heavy charged particles or multi-lepton events (52).

3. AMSB

A third class of SUSY models are those with anomaly-mediated SUSY-breaking (AMSB) (53; 54). These are extra dimensional scenarios in which SUSY is broken on another 3-dimensional subspace, and transmitted to our world through the conformal anomaly. As with all anomalies, this effect is one-loop suppressed. The fundamental scale of SUSY breaking as characterized by the gravitino mass is therefore $m_{\tilde{G}} \sim 10 - 100$ TeV, with MSSM sparticle masses one-loop suppressed and at the weak scale.

The AMSB contributions to sparticle masses are completely determined by the sparticle's gauge and Yukawa couplings. This leads to a highly predictive spectrum. Unfortunately, one of these predictions is $m_{\tilde{L}}^2, m_{\tilde{E}}^2 < 0$, but various mechanisms have been proposed to solve this tachyonic slepton problem; see, e.g., Refs. (55; 56; 57).

The gaugino masses are determined by the corresponding gauge group beta functions. In particular, AMSB predicts $M_1 : M_2 : M_3 \simeq 2.8 : 1 : 8$; because the SU(2) coupling is nearly scale-invariant in the MSSM, the Wino mass is the smallest. AMSB scenarios therefore motivate supersymmetric models with \tilde{W}^0 LSP and \tilde{W}^\pm NLSP. This triplet may be extremely degenerate, with the chargino traveling macroscopic distances before decaying to soft and invisible decay products, which provides a distinctive and challenging signature for collider searches (58).

D. Supersymmetric Higgs Bosons

The MSSM Higgs potential is

$$V_H = (m_{H_u}^2 + |\mu|^2)|H_u^0|^2 + (m_{H_d}^2 + |\mu|^2)|H_d^0|^2 - B(H_u^0 H_d^0 + \text{h.c.}) + \frac{1}{2}g^2|H_u^{0*} H_d^0|^2$$

$$+ \frac{1}{8}(g^2 + g'^2)(|H_u^0|^2 - |H_d^0|^2)^2, \quad (19)$$

where the parameters μ , $m_{H_u}^2$, and $m_{H_d}^2$ are as defined in Sec. II.B, and SUSY implies that all the quartic couplings are determined by the SU(2) and U(1) hypercharge gauge couplings, denoted g and g' , respectively. V_H automatically conserves CP, since any phase in the B parameter can be eliminated by a redefinition of the Higgs fields.

Assuming these parameters are such that the potential admits a stable, symmetry-breaking minimum, the three parameter combinations $m_{H_u}^2 + |\mu|^2$, $m_{H_d}^2 + |\mu|^2$, and B may be exchanged for the two vacuum expectation values $v_u \equiv \sqrt{2}\langle H_u^0 \rangle$, $v_d \equiv \sqrt{2}\langle H_d^0 \rangle$, and one physical Higgs boson mass, conveniently taken to be m_A . The W boson mass fixes $v_u^2 + v_d^2$, leaving one additional degree of freedom, usually taken to be $\tan \beta \equiv v_u/v_d$. Thus, at tree-level, the entire MSSM Higgs boson sector is determined by two parameters, m_A and $\tan \beta$.

In terms of these parameters, the physical Higgs boson masses are

$$m_{H_{\pm}}^2 = \frac{m_A^2 + m_Z^2 \pm \sqrt{(m_A^2 + m_Z^2)^2 - 4m_A^2 m_Z^2 c_{2\beta}^2}}{2} \quad (20)$$

$$m_{H^\pm}^2 = m_A^2 + m_W^2, \quad (21)$$

where $c_{2\beta} \equiv \cos 2\beta$. The CP-even mass eigenstates are related to the gauge eigenstates through

$$\begin{pmatrix} H \\ h \end{pmatrix} = \begin{pmatrix} \cos \alpha & \sin \alpha \\ -\sin \alpha & \cos \alpha \end{pmatrix} \begin{pmatrix} \sqrt{2} \text{Re} H_d^0 - v_d \\ \sqrt{2} \text{Re} H_u^0 - v_u \end{pmatrix}, \quad (22)$$

where the rotation angle α satisfies

$$\cos 2\alpha = -\cos 2\beta \frac{m_A^2 - m_Z^2}{m_H^2 - m_h^2} \quad (23)$$

with $-\pi/2 < \alpha < 0$.

Equation (20) implies that $m_h < m_Z |\cos 2\beta|$, a rather disastrous relation, given that experimental bounds exclude $m_h < m_Z$. The results presented so far, however, are valid only at tree-level. Large radiative corrections from top squark/quark loops (59),

$$\Delta m_h^2 \sim \frac{1}{\sin^2 \beta} \frac{3g^2 m_t^4}{8\pi^2 m_W^2} \log \frac{m_t^2}{m_t^2}, \quad (24)$$

can lift m_h to values above the experimental bounds. Note, however, that for $\tan \beta = 1$, $m_h = 0$ at tree-level, and so large values of m_h are not possible for $\tan \beta \approx 1$. From considerations of the Higgs mass alone, $\tan \beta < 1$ is possible. However, such values imply very large top Yukawa couplings, which become infinite well below the GUT or Planck scales. In addition, in simple frameworks, $\tan \beta < 1$ is incompatible with radiative electroweak symmetry breaking (60).

E. Neutralinos and Charginos

The neutralinos and charginos of the MSSM are the mass eigenstates that result from the mixing of the electroweak gauginos \tilde{B} and \tilde{W}^j with the Higgsinos.

The neutral mass terms are

$$\frac{1}{2}(\psi^0)^T M_N \psi^0 + \text{h.c.}, \quad (25)$$

where $(\psi^0)^T = (-i\tilde{B}, -i\tilde{W}^3, \tilde{H}_d^0, \tilde{H}_u^0)$ and

$$M_N = \begin{pmatrix} M_1 & 0 & -\frac{1}{2}g'v_d & \frac{1}{2}g'v_u \\ 0 & M_2 & \frac{1}{2}gv_d & -\frac{1}{2}gv_u \\ -\frac{1}{2}g'v_d & \frac{1}{2}gv_d & 0 & -\mu \\ \frac{1}{2}g'v_u & -\frac{1}{2}gv_u & -\mu & 0 \end{pmatrix}. \quad (26)$$

The neutralino mass eigenstates are $\tilde{\chi}_i^0 = \mathbf{N}_{ij}\psi_j^0$, where \mathbf{N} diagonalizes M_N . In order of increasing mass, the four neutralinos are labeled $\tilde{\chi}_1^0$, $\tilde{\chi}_2^0$, $\tilde{\chi}_3^0$, and $\tilde{\chi}_4^0$.

The charged mass terms are

$$(\psi^\pm)^T M_C \psi^\pm + \text{h.c.}, \quad (27)$$

where $(\psi^\pm)^T = (-i\tilde{W}^\pm, \tilde{H}^\pm)$ and

$$M_C = \begin{pmatrix} M_2 & \frac{1}{\sqrt{2}}gv_u \\ \frac{1}{\sqrt{2}}gv_d & \mu \end{pmatrix}. \quad (28)$$

The chargino mass eigenstates are $\tilde{\chi}_i^\pm = \mathbf{V}_{ij}\psi_j^\pm$ and $\tilde{\chi}_i^\mp = \mathbf{U}_{ij}\psi_j^\mp$, where the unitary matrices \mathbf{U} and \mathbf{V} are chosen to diagonalize M_C , and $\tilde{\chi}_1^\pm$ is lighter than $\tilde{\chi}_2^\pm$.

F. Sleptons

Sleptons are promising targets for colliders, as they are among the lightest sparticles in many models. As noted in Sec. II.A, sleptons include both left- and right-handed charged sleptons and sneutrinos. The mass matrix for the charged sleptons is

$$\begin{pmatrix} m_L^2 + m_\tau^2 - m_Z^2(\frac{1}{2} - s_W^2)c_{2\beta} & m_\tau(A_\tau - \mu \tan \beta) \\ m_\tau(A_\tau - \mu \tan \beta) & m_E^2 + m_\tau^2 - m_Z^2 s_W^2 c_{2\beta} \end{pmatrix} \quad (29)$$

in the basis $(\tilde{\tau}_L, \tilde{\tau}_R)$, where $s_W \equiv \sin \theta_W$. The sneutrino has mass

$$m_{\tilde{\nu}}^2 = m_L^2 + \frac{1}{2}m_Z^2 \cos 2\beta. \quad (30)$$

These masses are given in third-generation notation; in the presence of flavor mixing, these generalize to full six-by-six and three-by-three matrices.

The left-right mixing is proportional to lepton mass, and is therefore expected to be insignificant for selectrons and smuons, but may be important for staus, especially if $\tan \beta$ is large. Through level repulsion, this mixing lowers the lighter stau's mass. As noted in Sec. II.C, Yukawa couplings also lower scalar masses through renormalization group evolution. Both of these effects imply that in many scenarios, the lighter stau is the lightest slepton, and often the lightest sfermion.

G. Squarks

The mass matrix for up-type squarks is

$$\begin{pmatrix} m_Q^2 + m_t^2 + m_Z^2(\frac{1}{2} - \frac{2}{3}s_W^2)c_{2\beta} & m_t(A_t - \mu \cot \beta) \\ m_t(A_t - \mu \cot \beta) & m_U^2 + m_t^2 + m_Z^2 \frac{2}{3}s_W^2 c_{2\beta} \end{pmatrix} \quad (31)$$

in the basis $(\tilde{t}_L, \tilde{t}_R)$, and for down-type squarks is

$$\begin{pmatrix} m_Q^2 + m_b^2 - m_Z^2(\frac{1}{2} - \frac{1}{3}s_W^2)c_{2\beta} & m_b(A_b - \mu \tan \beta) \\ m_b(A_b - \mu \tan \beta) & m_D^2 + m_b^2 - m_Z^2 \frac{1}{3}s_W^2 c_{2\beta} \end{pmatrix} \quad (32)$$

in the basis $(\tilde{b}_L, \tilde{b}_R)$. Large mixing is expected in the stop sector, and possibly also in the sbottom sector if $\tan \beta$ is large. Because of these mixings and the impact of large Yukawa couplings in renormalization group evolution, the 3rd generation squarks are the lightest squarks in many models.

III. SEARCHES FOR MSSM NEUTRAL HIGGS BOSONS

As already explained in Sec. II, two Higgs doublets are needed in the MSSM to give mass to both up- and down-type quarks. Under the assumption that the Higgs sector is CP conserving, the physical states are two neutral CP-even Higgs bosons (h and H , ordered by increasing mass), a neutral CP-odd Higgs boson (A), and a doublet of charged Higgs bosons (H^\pm). Further details on the Higgs sector of the MSSM have been given in Sec. II. Here, we focus on searches for the neutral Higgs bosons of the MSSM, while searches for charged Higgs bosons will be discussed in Sec. IV.

A. MSSM benchmark scenarios

It has been seen that two parameters, commonly taken as m_A and $\tan \beta$, are sufficient to fully determine the MSSM Higgs sector at tree level, where $\tan \beta$ is the ratio of the vacuum expectation values of the Higgs fields giving mass to the up and down type quarks. Large radiative corrections, arising essentially from an incomplete cancellation of the top and stop loops, however modify the picture significantly. In particular, the important prediction $m_h < m_Z |\cos 2\beta|$ is invalidated. Among the many parameters of the MSSM, a few have been identified as being most relevant for the determination of the Higgs boson properties. In addition to m_A and $\tan \beta$, an effective SUSY breaking scalar mass, M_{SUSY} , which sets the scale of all squark masses, and a term controlling the amount of mixing in the stop sector, X_t , play the leading role. (In Eq. (24), the stop mass is directly related to M_{SUSY} , and stop mixing is neglected.) The model is further specified by a weak gaugino mass, M_2 , the gluino mass, $m_{\tilde{g}}$, and the SUSY Higgs mass term μ . The relation $X_t = A - \mu \cot \beta$ then allows the trilinear Higgs-squark coupling A (assumed to be universal) to

be calculated. For large values of $\tan\beta$, mixing in the sbottom sector becomes relevant too; it is controlled by $X_b = A - \mu \tan\beta$. Finally, the top quark mass m_t needs to be specified.

A few benchmark scenarios (61) were agreed upon to interpret the searches for MSSM Higgs bosons. The most widely considered are the so-called “ m_h -max” and “no-mixing” ones, where $M_{SUSY} = 1$ TeV, $M_2 = 200$ GeV, $\mu = -200$ GeV and $m_{\tilde{g}} = 800$ GeV. In m_h -max, X_t is set equal to $2M_{SUSY}$ (in the on-shell renormalization scheme), while it is set to 0 in the no-mixing scenario. The largest value of m_h is obtained for large m_A and $\tan\beta$, and is maximized (minimized) in the m_h -max (no-mixing) scenario. In the m_h -max scenario, the maximum value of m_h is $\simeq 135$ GeV.

B. Searches at LEP

At LEP, the neutral Higgs bosons of the MSSM have been searched for in two production processes, the Higgsstrahlung process $e^+e^- \rightarrow hZ$ and the associated production $e^+e^- \rightarrow hA$. Both processes are mediated by s -channel Z exchange. With the notations of Sec. II, the cross sections are

$$\sigma_{hZ} = \sin^2(\beta - \alpha)\sigma_{hZ}^{SM} \quad (33)$$

$$\sigma_{hA} = \cos^2(\beta - \alpha)\bar{\lambda}\sigma_{hZ}^{SM}, \quad (34)$$

where β and α are defined in Eqs. (14) and (22), and σ_{hZ}^{SM} is the production cross section for the SM Higgs boson. The parameter $\bar{\lambda}$ is the kinematic factor

$$\bar{\lambda} = \lambda_{hA}^{3/2} / [\lambda_{hZ}^{1/2} (12m_Z^2/s + \lambda_{hZ})], \quad (35)$$

where

$$\lambda_{ij} = [1 - (m_i + m_j)^2/s][1 - (m_i - m_j)^2/s], \quad (36)$$

and s is the square of the center-of-mass energy.

It is apparent from the above formulae that the two processes are complementary. In practice, the Higgsstrahlung process dominates for values of $\tan\beta$ close to unity, while associated production dominates for large values of $\tan\beta$, if kinematically allowed. In large regions of the MSSM parameter space, the h decay branching fractions are similar to those of the SM Higgs boson. For a mass of 115 GeV, these are 74% into $b\bar{b}$, 7% into both $\tau^+\tau^-$ and gg , 8% into WW^* , and 4% into $c\bar{c}$. The A boson couples only to fermions, so that its decay branching fraction into $b\bar{b}$ is always close to 90%, with most of the rest going into $\tau^+\tau^-$. Such branching fractions also hold for the h boson for large values of $\tan\beta$.

Searches for Higgs bosons were performed at LEP first in Z decays during the LEP1 era, and subsequently at increasing center-of-mass energies at LEP2, up to 209 GeV in 2000. In the following, only the searches performed at the highest energies are described.

The four LEP experiments carried out searches for the SM Higgs boson produced via Higgsstrahlung, and the

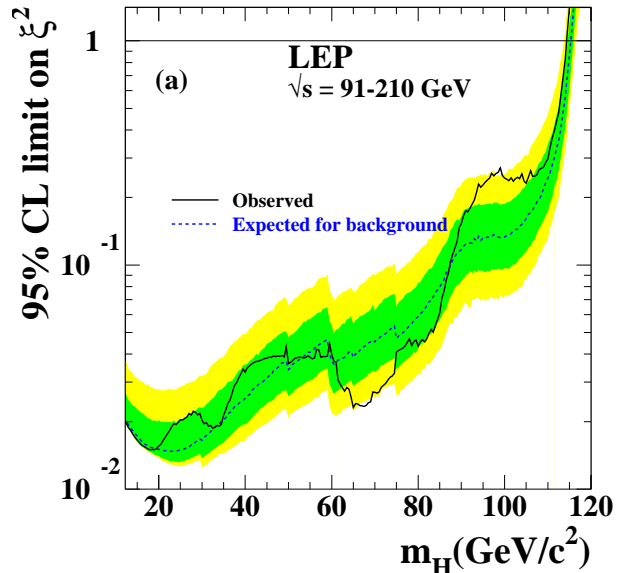


FIG. 3 The upper bound on the factor ξ^2 by which the square of the HZZ coupling is multiplied, as provided by the LEP experiments (62). The full curve is the observed limit, the dashed curve the median expected limit in the absence of signal, and the green and yellow bands are the 68% and 95% probability regions around the expected limit.

results were combined to maximize the sensitivity. (Production by vector boson fusion, $e^+e^- \rightarrow He^+e^-$ or $H\nu\bar{\nu}$, was also considered, but its contribution was found to be negligible in practice.) Four final state topologies were analyzed to cope with the various decay modes of the Higgs and Z bosons: a four-jet topology with two b -tagged jets, for $(H \rightarrow b\bar{b})(Z \rightarrow q\bar{q})$; a two b -tagged jets and two-lepton topology, for $(H \rightarrow b\bar{b})(Z \rightarrow \ell^+\ell^-)$, with $\ell = e$ or μ ; a two b -tagged jets and missing energy topology, for $(H \rightarrow b\bar{b})(Z \rightarrow \nu\bar{\nu})$; and a two-jet and two- τ topology for $(H \rightarrow b\bar{b})(Z \rightarrow \tau^+\tau^-)$ and $(H \rightarrow \tau^+\tau^-)(Z \rightarrow q\bar{q})$. A few candidate events were observed at the edge of the sensitivity domain, but the overall significance was only at the level of 1.7σ . A lower mass limit was therefore derived, excluding a SM Higgs boson with mass smaller than 114.4 GeV (62).

The Higgs boson mass lower limit depends on the strength of the HZZ coupling, and the LEP collaborations also provided, as a function of the mass of a SM-like Higgs boson, an upper limit on ξ^2 , where ξ is a multiplicative factor by which the SM HZZ coupling is reduced (62). By SM-like, it is meant that the decay branching fractions are similar to those expected from a SM Higgs boson. This result is shown in Fig. 3. Constraints on the MSSM parameter space can be deduced since in that case $\xi = \sin(\beta - \alpha)$.

For Higgs boson masses accessible at LEP, the structure of the MSSM Higgs sector is such that the h and A masses are similar whenever associated production is

relevant, i.e., for large values of $\tan\beta$. Searches for hA associated production were performed in the four b -jet final state for $(h \rightarrow b\bar{b})(A \rightarrow b\bar{b})$ and in the two b -jet and two- τ topology for $(h/A \rightarrow b\bar{b})(A/h \rightarrow \tau^+\tau^-)$. The constraint that the h and A candidate masses should be similar was imposed. The backgrounds from multijet and WW production were largely reduced by the b -jet identification requirements, leaving ZZ as an irreducible background.

No significant excess over the SM background expectation was observed, and production cross section upper limits were derived as a function of $m_h \simeq m_A$. For each benchmark scenario, a scan was performed as a function of m_A and $\tan\beta$, and in each point of the scan the cross section upper limit was compared to the corresponding prediction, taking into account the slight modifications expected for the values of the h and A branching fractions into $b\bar{b}$ and $\tau^+\tau^-$, as well as the non-negligible difference between m_h and m_A which develops at lower values of $\tan\beta$. If the cross section upper limit was found to be smaller than the prediction, the $(m_A, \tan\beta)$ set was declared excluded. The result of the combination of the searches in the hZ and hA channels by the four LEP experiments (63) is shown in Fig. 4, projected onto the $(m_h, \tan\beta)$ plane in the m_h -max and no-mixing scenarios. In the derivation of those results, occasional contributions of the $e^+e^- \rightarrow HZ$ and HA processes were taken into account.

In the most conservative scenario, i.e., m_h -max, it can be seen in Fig. 4 that the lower limit on the mass of the SM Higgs boson holds also for m_h as long as $\tan\beta$ is smaller than about 5, and that values of $\tan\beta$ below $\simeq 2$ are excluded for the current average value of the top quark mass, 172.6 ± 1.4 GeV (64). A lower mass limit of 93 GeV is obtained for $m_h \simeq m_A$ for large values of $\tan\beta$.

The benchmark scenarios were chosen such that the Higgs bosons do not decay into SUSY particles. An interesting possibility is that the $h \rightarrow \tilde{\chi}_1^0 \tilde{\chi}_1^0$ decay mode is kinematically allowed, where $\tilde{\chi}_1^0$ is the LSP. If R -parity is conserved, the LSP is stable and, since it is weakly interacting, the Higgs boson decay final state is invisible. Searches for such an “invisible” Higgs boson were performed by the LEP experiments, and the combination (65) yields a mass lower limit identical to that set on the SM Higgs boson if the production cross section is the SM one, as is the case for low values of $\tan\beta$.

To cope with fine-tuned choices of MSSM parameters, the LEP collaborations considered yet other possibilities, e.g., that the $h \rightarrow AA$ decay mode is kinematically allowed, or that the $h \rightarrow b\bar{b}$ decay is suppressed. For example, dedicated searches for $hA \rightarrow AAA \rightarrow b\bar{b}b\bar{b}$ and for hZ , with $h \rightarrow q\bar{q}$ in a flavor-independent way, have been performed (66). In the end, the sensitivity of the standard searches is only slightly reduced, except for rather extreme parameter choices leading, for instance, to $m_h \simeq 100$ GeV, while at the same time $m_A < 2m_b$. This last possibility is however less unnatural in extensions of the MSSM, such as the NMSSM where an additional

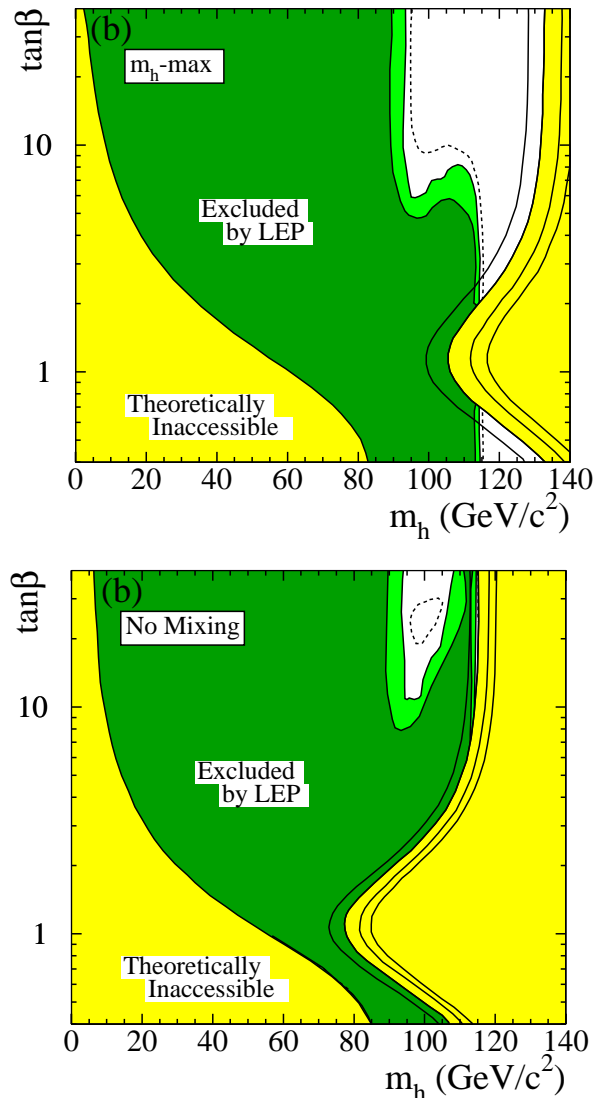


FIG. 4 Domains excluded at 95% CL (light green) and 99.7% CL (dark green) by the four LEP experiments (63) in the $(m_h, \tan\beta)$ plane within the m_h -max (top) and no-mixing (bottom) benchmark scenarios, with $m_t = 174.3$ GeV. The yellow regions are not accessible theoretically. The dashed lines represent the boundaries of the domains expected to be excluded at 95% CL in the absence of signal. The upper boundaries of the physical regions are indicated for four top quark masses: 169.3, 174.3, 179.3, and 183 GeV, from left to right.

Higgs singlet field is introduced (67).

Finally, the possibility that CP be not conserved in the Higgs sector was also considered. While CP is conserved at tree level, radiative corrections may introduce such a CP violation if the relative phase of μ and A is not vanishing. In such a case, the three mass eigenstates all share properties of h , H and A , so that the signatures of Higgs boson production are less distinct. The constraints are accordingly weaker. A dedicated “CPX” scenario (68) was set up to perform quantitative studies. As an ex-

ample, a region around $m_h = 45$ GeV and $\tan\beta = 5$ is not excluded for $M_{SUSY} = 500$ GeV, $M_2 = 200$ GeV, $\mu = 2$ TeV, and $m_{\tilde{g}} = 1$ TeV, when $|A| = 1$ TeV and $\arg(A) = 90^\circ$. Further details can be found in Ref. (63).

C. Searches at the Tevatron

At the Tevatron, i.e., in $p\bar{p}$ collisions at 1.96 TeV, the dominant production mechanism for the SM Higgs boson is via gluon fusion, $gg \rightarrow H$. In the mass range that is of interest for a SM-like Higgs boson of the MSSM, namely $m_h < 135$ GeV, the dominant decay mode is $H \rightarrow b\bar{b}$. Such a two-jet final state is totally overwhelmed by standard jet production via the strong interaction, even after b -jet identification. This is why the SM Higgs boson searches at the Tevatron have been performed in the associated production processes $q\bar{q} \rightarrow (W/Z)H$, which proceed via s -channel W or Z exchanges in a similar way to the Higgsstrahlung in e^+e^- collisions. In spite of cross sections an order of magnitude smaller than that of gluon fusion, these processes offer better discrimination against the multijet background, by making use of the leptonic decays of the W and Z ($W \rightarrow l\nu$, $Z \rightarrow l^+l^-$ and $Z \rightarrow \nu\bar{\nu}$). These searches for the SM Higgs boson apply equally well for the h boson of the MSSM in the low $\tan\beta$ regime. Their sensitivity is, however, still not sufficient to provide any significant constraint.

The situation is much more favorable for large values of $\tan\beta$. In this regime, two Higgs bosons are almost mass degenerate, h and A or H and A , depending on whether m_A is less than or greater than m_h^{max} , where m_h^{max} is the maximum value that m_h can take, e.g., 135 GeV in the m_h -max scenario. In the following, these two Higgs bosons are collectively denoted ϕ . Their couplings to b quarks and τ leptons are enhanced by a factor $\tan\beta$ with respect to the SM couplings. As a result, the contribution of the b quark loop to their production via gluon fusion is enhanced by a factor $2\tan^2\beta$. Although this is not sufficient to render feasible a detection in the $\phi \rightarrow b\bar{b}$ decay mode, this is not the case for the $\phi \rightarrow \tau^+\tau^-$ decay mode, the branching fraction of which amounts to $\simeq 10\%$.

One of the two τ s is required to decay leptonically ($\tau \rightarrow (e/\mu)\nu$) to ensure proper triggering. Three final state topologies are considered: $e\tau_{had}$, $\mu\tau_{had}$, and $e\mu$, all with missing transverse energy \cancel{E}_T from the τ decay neutrinos. Here τ_{had} denotes a τ lepton decaying into hadrons and a neutrino. The dominant, irreducible background comes from Z production with $Z \rightarrow \tau^+\tau^-$, but there also remains a substantial component from $(W \rightarrow l\nu)+jet$, where the jet is misidentified as a τ . This background is reduced, for instance, by requiring a low transverse mass of the lepton and the \cancel{E}_T . The final discriminating variable is the visible mass $m_{vis} = \sqrt{(P_{\tau_1} + P_{\tau_2} + \cancel{E}_T)^2}$, constructed from the τ visible products and from the \cancel{E}_T . The distribution of m_{vis} obtained by CDF (69) in a 1.8 fb^{-1} data sample is shown in Fig. 5. From this distribution, as well as from a simi-

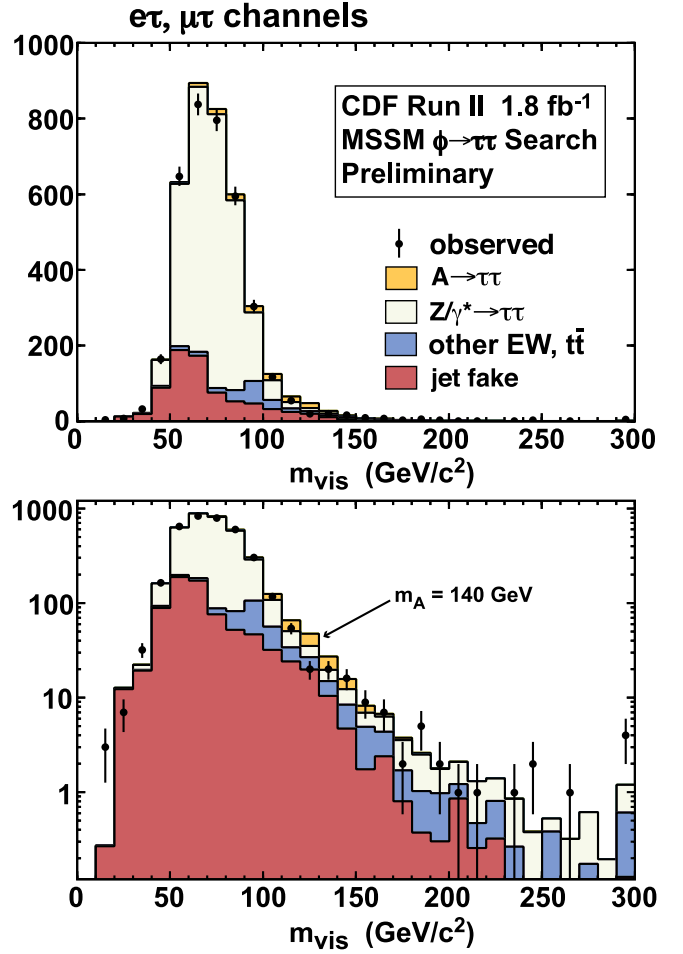


FIG. 5 Visible mass distribution in the $(e/\mu)\tau_{had}$ channels from the CDF search for $\phi \rightarrow \tau\tau$ (69). The signal contribution indicated corresponds to the cross section upper limit set with this data.

lar one in the $e\mu$ channel, a cross section upper limit on ϕ production is derived, which in turn is translated into exclusion domains in the $(m_A, \tan\beta)$ plane within benchmark scenarios. The result obtained in the m_h -max and no-mixing scenarios is shown in Fig. 6. Similar results have been obtained by DØ (70).

Because of the enhanced coupling of ϕ to b quarks at high $\tan\beta$, the production of Higgs bosons radiated off a b quark may be detectable in the $\phi \rightarrow b\bar{b}$ decay mode in spite of the large background from multijet events produced via the strong interaction (“QCD background”). This process can be described in the so-called four-flavor or five-flavor schemes, and it has been shown that the two approaches yield very similar results (71). In the four-flavor scheme, the main contribution comes from gluon fusion, $gg \rightarrow b\bar{b}\phi$, while the main one in the five-flavor scheme comes from $gb \rightarrow b\phi$. Because one of the final state b quarks (a spectator b quark in the five-flavor scheme) tends to be emitted with a low transverse momentum, the searches require only three b jets to be identified. The signal is searched by inspection of the mass

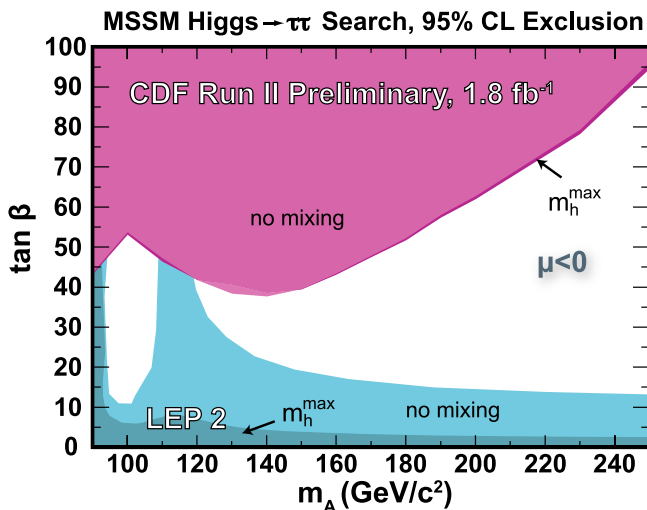


FIG. 6 Domains in the $(m_A, \tan\beta)$ plane excluded by the CDF search for $\phi \rightarrow \tau\tau$ (69). The domains excluded at LEP are also indicated.

distribution of the two jets with highest transverse momenta in the sample of events with three b -tagged jets. Further discrimination against the QCD background is provided by the mass of the charged particles in the tagged jets (at CDF (72)) or by the inclusion of additional kinematic variables in a likelihood discriminant (at DØ (73)). The QCD background is modeled using a combination of information from control samples in the data, where one of the jets is not b tagged, and from Monte Carlo simulations of the various processes contributing to the background (bbb , bbc , bbq , ccc , ccq , etc., where q represents a light quark, u , d , s , or a gluon). The mass distribution obtained by CDF in a 1.9 fb^{-1} data sample is shown in Fig. 7, with the individual background contributions displayed. No signal was observed, and production cross section upper limits were derived, from which exclusion domains in the $(m_A, \tan\beta)$ plane were determined in various benchmark scenarios. The DØ result obtained with 2.6 fb^{-1} in the m_h -max scenario is shown in Fig. 8. In the derivation of the cross section upper limits and exclusion domains, special attention was given to a proper handling of the Higgs boson width, which is enhanced by a factor $\tan^2\beta$ at tree level and therefore becomes large with respect to the mass resolution. (This was not the case for $\phi \rightarrow \tau^+\tau^-$ because of the degradation of the mass resolution due to the missing neutrinos.). It should also be noted that the exclusion domain is quite sensitive to the model parameters. It is smaller in the no-mixing scenario, and also if the sign of μ is chosen positive. These effects due to potentially large SUSY loop corrections to the production cross sections and decay widths tend to cancel in the search for $\phi \rightarrow \tau^+\tau^-$ described above (74).

Finally, Higgs bosons produced in association with b quarks can also be searched for in the $\phi \rightarrow \tau^+\tau^-$ decay mode. Although the branching fraction is an order of magnitude smaller than the one of $\phi \rightarrow b\bar{b}$, the signal

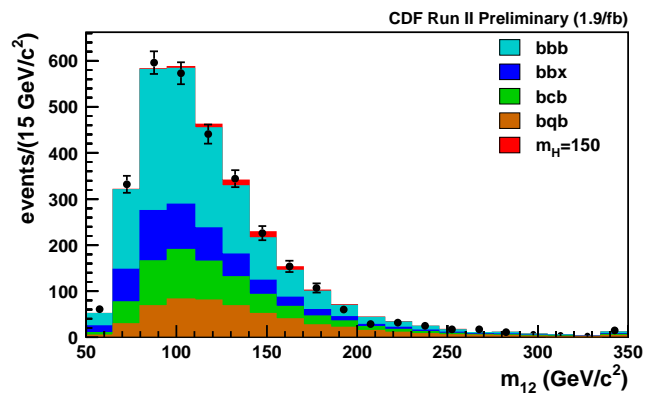


FIG. 7 Fit to the mass of the two jets with highest transverse momenta in the CDF sample of events with three b -tagged jets (72). The contributions of the various multijet backgrounds and of a signal with a mass of 150 GeV are indicated.

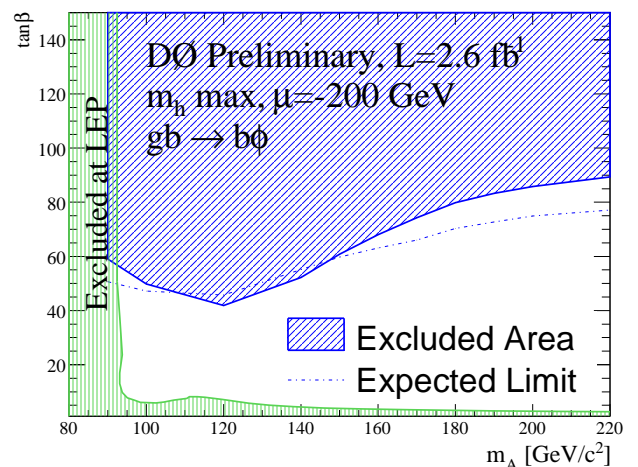


FIG. 8 Domain in the $(m_A, \tan\beta)$ plane excluded by the DØ search for $\phi \rightarrow b\bar{b}$ in events with three b -tagged jets in the m_h -max scenario (73).

is much easier to disentangle from the background. A DØ analysis (75) was performed where one of the τ s decays into a muon and neutrinos, while the other decays into hadrons and a neutrino. Furthermore, a b -tagged jet was required, at which point the main background comes from top quark pair production, $t\bar{t} \rightarrow \mu\nu b\tau\nu\bar{b}$. A neural network was used to discriminate signal and $t\bar{t}$ background, taking advantage of the large differences in their kinematic properties. The result, based on 1.2 fb^{-1} is shown in Fig. 9. Given the limited amount of integrated luminosity used up to now, this channel appears to be quite promising.

IV. SEARCHES FOR CHARGED HIGGS BOSONS

Many extensions of the SM involve more than one complex doublet of Higgs fields. Two-Higgs doublet mod-

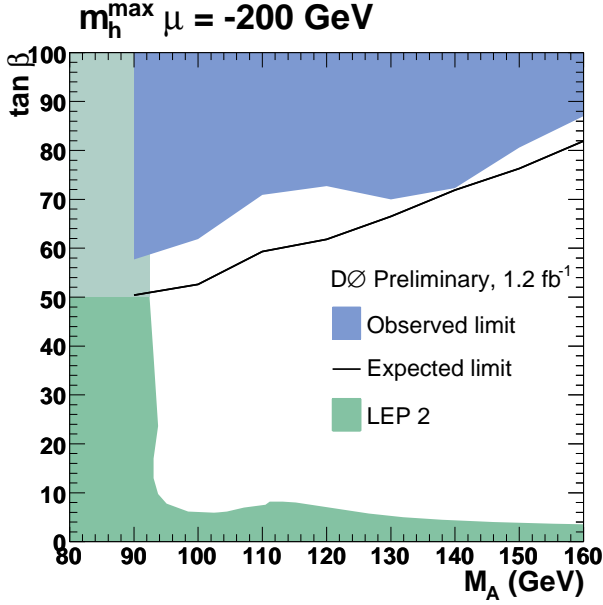


FIG. 9 Domain in the $(m_A, \tan \beta)$ plane excluded by the D0 search for $\phi \rightarrow \tau^+\tau^-$ produced in association with a b quark in the m_h -max scenario (75). The light green shaded region is the extension of the LEP exclusion region to $\tan \beta > 50$.

els (2HDMs) fall into three main categories. In Type I models, all quarks and leptons couple to the same Higgs doublet. In Type II models, down-type fermions couple to the first Higgs doublet, and up-type fermions couple to the second Higgs doublet. Flavor-changing neutral currents are naturally avoided in Type I and Type II 2HDMs. In Type III models, fermions couple to both doublets, and flavor-changing neutral currents must be avoided using other strategies. In addition to the three neutral Higgs bosons discussed in the previous section, 2HDMs involve a pair of charged Higgs bosons, H^\pm . Most of the experimental results on charged Higgs bosons have been obtained within the context of Type II 2HDMs, of which the MSSM is a specific instance.

In Type II 2HDMs, the charged Higgs boson decay width into a fermion pair $\bar{f}_u f_d$ is

$$\Gamma(H^- \rightarrow \bar{f}_u f_d) = \frac{N_c g^2 m_{H^\pm}}{32\pi m_W^2} \left(1 - \frac{m_{f_u}^2}{m_{H^\pm}^2}\right)^2 \times (m_{f_d}^2 \tan^2 \beta + m_{f_u}^2 \cot^2 \beta), \quad (37)$$

where N_c is the number of colors, and we have approximated $m_{f_d} \ll m_{H^\pm}$ in the phase space factor. Charged Higgs bosons therefore decay into the heaviest kinematically-allowed fermions: $\tau^-\bar{\nu}_\tau$ at large $\tan \beta$ and $\bar{c}s$ at low $\tan \beta$ for charged Higgs boson masses to which current accelerators are sensitive.

A. Searches at LEP

At LEP, charged Higgs bosons are produced in pairs as $e^+e^- \rightarrow H^+H^-$. The production cross section depends only on SM parameters and on the mass of the charged Higgs boson. The process $e^+e^- \rightarrow H^+W^-$ has a significantly lower cross section.

The charged Higgs boson can decay into $c\bar{s}$ or $\tau\nu_\tau$. In searches for Type I 2HDM Higgs bosons, the decay $H^\pm \rightarrow AW^{\pm*}$ is also considered, as in Refs. (76; 77). The interpretation of the search results generally assumes that $\text{Br}(H^\pm \rightarrow \tau\nu_\tau) + \text{Br}(H^\pm \rightarrow qq') = 1$, where the dominant qq' flavors are $c\bar{s}$, due to CKM suppression of $\bar{c}b$. This assumption leads to the consideration of three topologies for pair-produced charged Higgs bosons: four jets from $H^+H^- \rightarrow c\bar{s}c\bar{s}$, two jets, a τ lepton and missing energy from $H^+H^- \rightarrow c\bar{s}\tau\bar{\nu}_\tau$ and two charge conjugate, acoplanar¹ τ leptons from $H^+H^- \rightarrow \tau^+\nu_\tau\tau^-\bar{\nu}_\tau$.

Direct searches for pair production of charged Higgs bosons have been published by all four LEP experiments (76; 77; 78; 79). Each topological analysis begins with a general selection for the expected number of jets and taus, followed by more sophisticated techniques. The main difficulty in these analyses is separating the signal from the nearly identical signature of W^+W^- production; selection criteria usually include a mass-dependent optimization. Techniques such as linear discriminants, likelihood estimators, and jet-flavor tagging are used in these analyses. The $H^+H^- \rightarrow \tau^+\nu_\tau\tau^-\bar{\nu}_\tau$ channel has additional complexity due to the missing neutrinos, which removes the possibility of reconstructing the H^\pm candidate masses and of improved discrimination from the equal-mass constraint. However, final states with taus can benefit from extracting information about the tau polarization; the τ^+ from a H^+ (a scalar) is produced in a helicity state opposite to that of a τ^+ from W^+ decay.

The LEP experiments have combined the results of their searches for charged Higgs bosons into one result (80) based on common assumptions. The total dataset has an integrated luminosity of 2.5 fb^{-1} , collected at center-of-mass energies between 189 and 209 GeV. The possible decays are restricted to $H^+ \rightarrow c\bar{s}$ and $\tau^+\nu_\tau$ in a general 2HDM framework. The combined mass limit is shown in Fig. 10 as a function of $\text{Br}(H^+ \rightarrow \tau^+\nu_\tau)$. A lower bound of 78.6 GeV holds for any value of the branching ratio.

B. Searches at the Tevatron

At the Tevatron, pair production of charged Higgs bosons is expected to occur at a very low rate. How-

¹ The acoplanarity angle is the angle between the projections of the τ momenta on a plane transverse to the beam axis. If this angle is less than 180° , the τ leptons are said to be acoplanar.

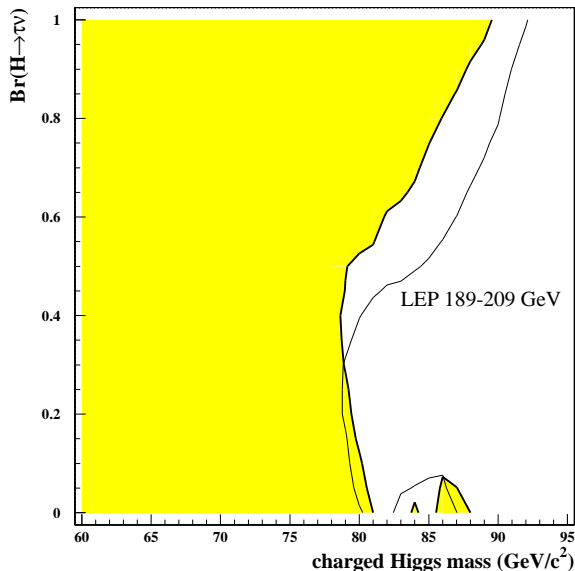


FIG. 10 Limit on the charged Higgs boson mass as a function of $\text{Br}(H^+ \rightarrow \tau^+ \nu_\tau)$, from the combined data of the four LEP experiments at center-of-mass energies from 189 to 209 GeV. The expected exclusion limit is shown as a thin solid line and the observed limit as a thick solid line; the shaded region is excluded (80).

ever, in contrast to searches at LEP, advantage can be taken of the large mass of the top quark, which opens new ways to search for evidence of charged Higgs bosons. Two approaches are considered, depending on whether the charged Higgs boson is lighter or heavier than the top quark. In the first case, the top quark can decay into H^+ and a b quark. For heavier charged Higgs bosons, resonant production of a single H^+ followed by the decay $H^+ \rightarrow t\bar{b}$ is the most promising process.

In the SM, the top quark decays almost exclusively into a W and a b quark, and the possible signatures of $t\bar{t}$ pair production are associated with the various combinations of W -boson decay channels. If the charged Higgs boson is lighter than the top quark, the decay $t \rightarrow H^+ b$ will compete with the standard $t \rightarrow W^+ b$ mode. The decay of the charged Higgs boson, with branching ratios different from those of the W , will modify the fractions of events observed in the various topologies, compared to the SM expectations.² The qualitative aspects and magnitude of these modifications depend on the model parameters. The dependence on $\tan\beta$ of the top quark decay ratio to $H^+ b$ and of the various charged-Higgs boson decay

² The branching ratios for topologies arising from SM $t\bar{t}$ pair production are roughly 50% in six jets; 14% in each of e, μ , and $\tau + 4$ jets + \cancel{E}_T ; 1% in each of $ee, \mu\mu$, and $\tau\tau + 2$ jets + \cancel{E}_T ; and 2% in each of $e\mu, e\tau$, and $\mu\tau + 2$ jets + \cancel{E}_T . In each of these channels, there are two b jets.

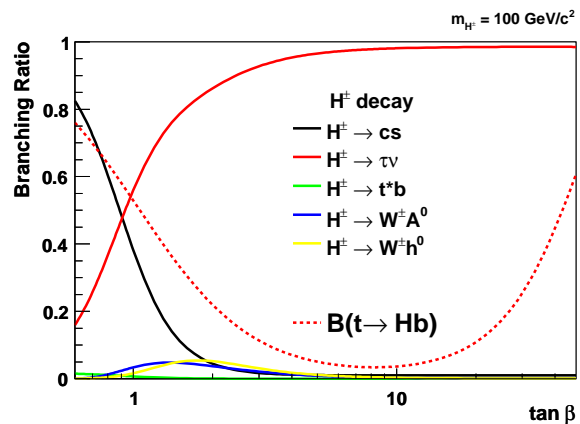


FIG. 11 For a charged Higgs boson mass of 100 GeV, the branching ratios for the top quark decay into $H^+ b$, under the assumption that $\text{Br}(t \rightarrow W^+ b) + \text{Br}(t \rightarrow H^+ b) = 1$, and for the various H^+ decay channels, as a function of $\tan\beta$. From Ref. (81).

channels is shown in Fig. 11 for $m_{H^+} = 100$ GeV and a typical set of MSSM parameters, with QCD, SUSY-QCD and electroweak radiative corrections to the top and bottom quark Yukawa couplings calculated with the CPsuperH code (82). The dominant H^+ decay channels are $c\bar{s}$ or $\tau^+ \nu_\tau$ at low and high values of $\tan\beta$, respectively; with this set of parameters, H^+ decays to $W^+ A/h$ are also allowed, although always at a small rate. The $H^+ \rightarrow t^* \bar{b} \rightarrow W^+ b\bar{b}$ decay mode becomes relevant for charged Higgs boson masses closer to the top quark mass. It can be seen that charged Higgs bosons will be most prominent at high and low values of $\tan\beta$. Two simplified models address each of these regions: the tauonic model, with $\text{Br}(H^+ \rightarrow \tau^+ \nu_\tau) = 1$, and the leptophobic model, with $\text{Br}(H^+ \rightarrow c\bar{s}) = 1$. The tauonic model is a very good approximation in the MSSM for $\tan\beta \gtrsim 15$, while purely leptophobic charged Higgs bosons can be found in some multi-Higgs-doublet models (83).

Analyses based on measurements of $t\bar{t}$ final states include an earlier CDF search in 200 pb^{-1} of data (84) and a recent DØ analysis of 1 fb^{-1} of data (81). The yields observed in the various topologies are compared to what would be expected in models with charged Higgs bosons, taking into account the $t \rightarrow H^+ b$ and H^\pm decay branching ratios predicted as a function of the Higgs boson mass and $\tan\beta$. In particular, no excess of final states involving τ leptons is observed, nor any disappearance of final states with one or two leptons, jets and \cancel{E}_T , as would be expected at large and small $\tan\beta$, respectively. Figure 12 displays the exclusion domain in the plane of the charged Higgs boson mass and $\tan\beta$ from the DØ analysis (81), for leptophobic and tauonic models. The CDF analysis excludes $\text{Br}(t \rightarrow H^+ b) > 0.4$ for a tauonic H^\pm (84).

In a recent analysis based on a data sample of 2.2 fb^{-1} , the CDF collaboration used a different approach to search for a leptophobic charged Higgs boson in top quark decays (85). The search is performed in the

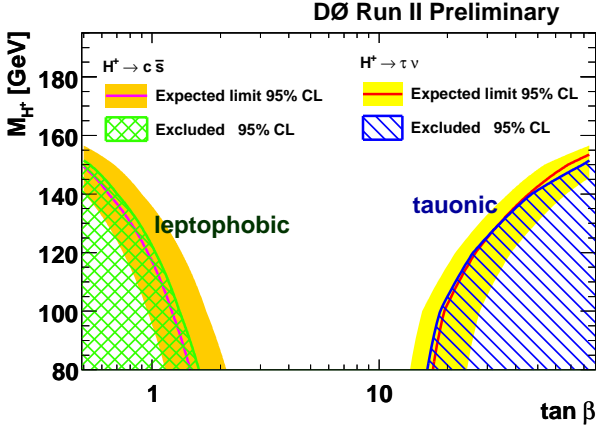


FIG. 12 Limit on the mass of the charged Higgs boson as a function of $\tan \beta$ from the DØ search in top quark decays (81).

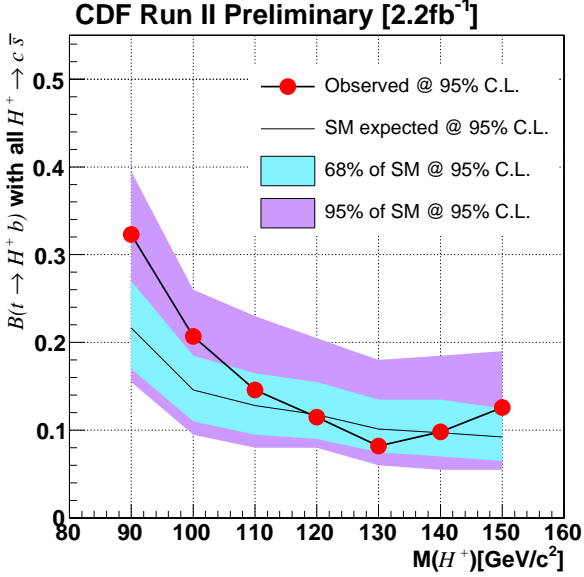


FIG. 13 For a leptophobic charged Higgs boson, upper limit on the branching ratio $\text{Br}(t \rightarrow H^+ b)$ as a function of the Higgs boson mass from a CDF search in top quark decays (85).

lepton + jets + \cancel{E}_T final states with two b -tagged jets, where the lepton (electron or muon), the neutrino (responsible for the missing E_T), and a b jet are the signature of a $t \rightarrow Wb \rightarrow \ell\nu b$ decay, while the other top quark of the $t\bar{t}$ pair is assumed to decay to either $Wb \rightarrow q\bar{q}b$ or $Hb \rightarrow c\bar{s}b$. The $t\bar{t}$ event is fully reconstructed, taking the masses of the W boson and of the top quark into account as constraints to assign correctly each of the b jets to its parent t or \bar{t} . Templates of the mass of the dijet system reconstructed from the non- b jets are used to extract limits on the branching ratio of $t \rightarrow H^+ b$, as shown in Fig. 13.

If the charged Higgs boson is heavier than the top quark, it will decay dominantly into $t\bar{b}$. The resonant production of such a charged Higgs boson leads to a

final state similar to the one resulting from single top s -channel production, $q\bar{q} \rightarrow W^* \rightarrow t\bar{b}$. Therefore the analyses developed for the search for single top production can be applied to the search for a charged Higgs boson. Such an analysis was performed by the DØ collaboration (86), in the topology arising from a subsequent $t \rightarrow Wb \rightarrow \ell\nu b$ decay. The large H^\pm mass, reconstructed from the decay products imposing the W and top mass constraints, is used as discriminating variable. No excess is observed over SM background predictions, and upper limits are set on the production of a charged Higgs boson. The results are however not sensitive to Type II 2HDMs, but provide some exclusion in a Type I 2HDM.

V. SEARCHES FOR SUPERSYMMETRIC PARTICLES

A. General features of SUSY models

As explained in Sec. II, the main features of SUSY models for phenomenology are related to the type of mediation mechanism for SUSY breaking, to the choice of soft breaking terms, and to whether or not R -parity is assumed to be conserved.

The most widely studied models involve gravity-mediation of SUSY breaking. In the minimal form of such models, mSUGRA, R -parity is conserved, and only five parameters are needed beyond those already present in the standard model: a universal gaugino mass $m_{1/2}$, a universal scalar mass m_0 , and a universal trilinear coupling A_0 , all defined at the scale of grand unification, and $\tan \beta$ and the sign of μ . The low energy parameters, including $|\mu|$, are determined by the renormalization group equations and by the condition of electroweak symmetry breaking. In addition, it is commonly assumed that the LSP is the lightest neutralino $\tilde{\chi}_1^0$. A somewhat less constrained model keeps μ and m_A as independent low energy parameters, which is in effect equivalent to decoupling the Higgs sector from the other scalars. Such a model was largely used at LEP.

Many studies have been performed where the assumption of R -parity conservation is dropped, while keeping unchanged the other features of those mSUGRA inspired models. If R -parity is violated, the superpotential is allowed to contain lepton or baryon number-violating terms (87)

$$W_{R_p} = \lambda_{ijk} L_i L_j \bar{E}_k + \lambda'_{ijk} L_i Q_j \bar{D}_k + \lambda''_{ijk} \bar{U}_i \bar{D}_j \bar{D}_k, \quad (38)$$

where L and Q are lepton and quark doublet superfields, E and D are lepton and down-type quark singlet superfields, and i, j and k are generation indices. These terms are responsible for new couplings through which the LSP decays to SM particles. The simultaneous occurrence of different coupling types is however strongly constrained, e.g., by the bounds on the proton lifetime, which is why it is commonly assumed that only one of the R -parity violating terms is present in the superpotential.

In models with gauge-mediated SUSY breaking (GMSB), the LSP is a very light gravitino \tilde{G} , and the phenomenology is governed by the nature of the NLSP. In the minimal such model, mGMSB, all SUSY particle masses derive from a universal scale Λ , and in most of the parameter space the NLSP is either the lightest neutralino $\tilde{\chi}_1^0$ or the lighter stau $\tilde{\tau}_R$, the latter occurring preferentially at large $\tan\beta$. The couplings of the gravitino depend on yet another parameter, the SUSY-breaking scale \sqrt{F} , which can be traded for the lifetime of the NLSP.

Anomaly-mediation of SUSY breaking (AMSB) generically leads to a neutralino LSP which is almost a pure wino \tilde{W}^0 , and has a small mass splitting with the lighter chargino. As a consequence, this chargino may acquire a phenomenologically relevant lifetime, possibly such that it behaves like a stable particle.

B. Signatures and strategies

Most of the searches for SUSY particles were performed within a “canonical scenario,” the main features of which are borrowed from mSUGRA: R -parity conservation, universal gaugino mass terms, a universal sfermion mass term, and a neutralino LSP. Because of R -parity conservation, SUSY particles are produced in pairs, and each of the produced SUSY particles decays into SM particles accompanied by an LSP. Since the LSP is neutral and weakly interacting, it appears as missing energy, which is the celebrated signature of SUSY particle production.

Alternatively, if R -parity is not conserved, the LSP decays to SM particles, so that no missing energy is expected beyond that possibly arising from neutrinos. The signature of SUSY particle production is therefore to be sought in an anomalously large multiplicity of jets or leptons. The R -parity violating couplings can also make it possible that SUSY particles are produced singly, rather than in pairs.

In R -parity conserving scenarios other than the canonical one, additional or different features are expected. In GMSB, each of the pair-produced SUSY particles decays into SM particles and an NLSP. The NLSP further decays into its SM partner and a gravitino. With a neutralino NLSP in the mass range explored up to now, the dominant decay is $\tilde{\chi}_1^0 \rightarrow \gamma\tilde{G}$, so that the final state contains photons, with missing energy due to the escaping gravitinos. With a stau NLSP, the decay is $\tilde{\tau}_R \rightarrow \tau\tilde{G}$. If the stau lifetime is so long that it escapes the detector before decaying, the final state from stau pair production does not exhibit any missing energy, but rather appears as a pair of massive stable particles. A similar final state may also arise from chargino pair production in AMSB. Long-lived gluinos can lead to spectacular signatures if they are brought to rest by energy loss in the detector material.

Except for the gluino, all SUSY particles are produced

in a democratic way in e^+e^- collisions via electroweak interactions. It is therefore natural that the searches at LEP were targeted toward the lightest ones. The results of these searches could further be combined within a given model, thus providing constraints on the model parameters. In contrast, it is expected that the most copiously produced SUSY particles in hadron collisions, such as $p\bar{p}$ at the Tevatron, will be colored particles, namely squarks and gluinos. Their detailed signature however depends on the mass pattern of the other SUSY particles, which may be present in their decay chains. This is why a specific model, usually mSUGRA, is needed to express the search results in terms of mass constraints. Thanks to lower masses and more manageable backgrounds, the search for gauginos produced via electroweak interactions can be competitive at hadron colliders for model parameter configurations where their leptonic decays are enhanced.

In e^+e^- collisions, the production cross sections of SUSY particles are similar to those of their SM partners, except for the phase space reduction due to their larger masses. The data collected at the highest LEP energies, up to 209 GeV, are therefore the most relevant for SUSY particle searches. Mixing effects may however reduce these cross sections, as is the case for instance for neutralinos with a small Higgsino component, in which case the large integrated luminosity accumulated by the LEP experiments at lower energies also contributes to the search sensitivity.

Although the center-of-mass energy of 1.96 TeV in $p\bar{p}$ collisions at the Tevatron allows higher new particle masses to be probed, large integrated luminosities are needed because of the rapid PDF fall off at high x , as explained in Sec. I.B. The search for SUSY particles at the Tevatron is also rendered more challenging than at LEP because of the large cross sections of the background processes. In the searches for squarks and gluinos, signal production cross sections of the order of 0.1 pb at the edge of the sensitivity domain are to be compared to the total inelastic cross section of 80 mb. In the searches for gauginos, with similar signal production cross sections in the mass range probed, the main backgrounds are $W \rightarrow \ell\nu$ and $Z \rightarrow \ell\ell$, with cross sections at the 2.7 nb and 250 pb level per lepton flavor.

In ep collisions at the HERA collider, the most promising SUSY particle production process was single squark resonant production via an R -parity violating λ'_{1j1} or λ'_{11k} coupling, with a cross section depending not only on the squark mass, but also on the value of the coupling involved. The decay of the squark produced could be either direct, via the same λ' coupling as for its production, or indirect through a cascade leading to the LSP, which in turn decays to two quarks and a neutrino or an electron. The mass reach at HERA was the full center-of-mass energy of 320 GeV, but the production of squarks with masses close to this bound involved quarks at large x values, so that the effective reach was substantially smaller, even for large values of the λ' coupling.

C. Searches in the canonical scenario

As mentioned above, the characteristic signature of SUSY particle production in the canonical scenario is missing energy carried away from the detector by the LSPs at the end of the decay chains.

1. Searches at LEP

Sleptons: In e^+e^- annihilation, the search for SUSY particles that involves the least set of hypotheses for its interpretation is the search for smuons. Pair production proceeds via Z/γ^* exchange in the s -channel. Because of the small mass of the muon, the smuon mass eigenstates can be identified with the interaction eigenstates, of which $\tilde{\mu}_R$ is the lighter one in models with slepton and gaugino mass unification. The search results were interpreted under this assumption, which is furthermore conservative, as the coupling of the $\tilde{\mu}_R$ to the Z is smaller than that of the $\tilde{\mu}_L$. Only one parameter is needed to calculate the smuon pair production cross section, the smuon mass $m_{\tilde{\mu}_R}$. The sole decay mode of a $\tilde{\mu}_R$ NLSP is $\tilde{\mu}_R \rightarrow \mu\tilde{\chi}_1^0$, so that smuon pair production leads to a final state consisting of two acoplanar muons with missing energy and momentum. The topology of this final state also depends on the mass of the LSP. If $m_{\tilde{\chi}_1^0}$ is small, the final state is very similar to that arising from W pair production, with both W bosons decaying to a muon and a neutrino. If the $\tilde{\mu}_R - \tilde{\chi}_1^0$ mass difference is small, the final state muons carry little momenta, so that the selection efficiency is reduced. In that configuration, the main background comes from “ $\gamma\gamma$ interactions,” $e^+e^- \rightarrow (e^+)\gamma^*\gamma^*(e^-) \rightarrow (e^+)\mu^+\mu^-(e^-)$, where the spectator electrons (e^\pm) escape undetected in the beam pipe. The LSP mass $m_{\tilde{\chi}_1^0}$ is therefore needed, in addition to the smuon mass, to interpret the search results. The constraints obtained in the $(m_{\tilde{\mu}_R}, m_{\tilde{\chi}_1^0})$ plane by the four LEP experiments (88) are shown in Fig. 14. If the assumption that the smuon is the NLSP is dropped, further specification of the model is needed to turn the search results into mass constraints. An example is shown in Fig. 14 in the case of gaugino mass unification, for the specified values of μ and $\tan\beta$. A slight reduction of the excluded domain is observed for low values of $m_{\tilde{\chi}_1^0}$, due to the competition of the $\tilde{\mu}_R \rightarrow \mu\tilde{\chi}_2^0$ decay mode, with $\tilde{\chi}_2^0 \rightarrow \gamma\tilde{\chi}_1^0$. Depending on $m_{\tilde{\chi}_1^0}$, smuon masses smaller than 95 to 99 GeV are excluded, except for $\tilde{\mu}_R - \tilde{\chi}_1^0$ mass differences below 5 GeV.

Because of the larger τ mass, compared to the muon mass, the hypothesis that the stau mass eigenstates can be identified with the interaction eigenstates may not hold, especially for large values of $\tan\beta$ that enhance the off-diagonal elements of the mass matrix in Eq. (29). The coupling to the Z of the lighter stau mass eigenstate $\tilde{\tau}_1$ may therefore be reduced with respect to the smuon coupling to the Z , and even vanish. Moreover, because there is at least one neutrino in each τ decay, the visible

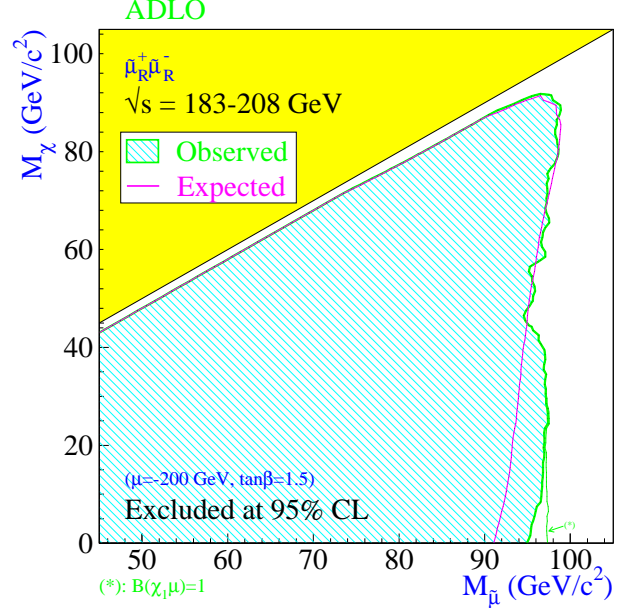


FIG. 14 Region in the $(m_{\tilde{\mu}_R}, m_{\tilde{\chi}_1^0})$ plane excluded by the searches for smuons at LEP (88). The dotted contour is drawn under the assumption that the smuon decay branching ratio into $\mu\tilde{\chi}_1^0$ is 100%.

energy of the final state arising from stau pair production is smaller than in the case of smuons, so that the selection efficiency is reduced. The mass lower limits obtained at LEP are therefore lower for staus than for smuons, from 86 to 95 GeV, depending on $m_{\tilde{\chi}_1^0}$, provided the $\tilde{\tau}_1 - \tilde{\chi}_1^0$ mass difference is larger than 7 GeV (88).

As for smuons, the selectron mass eigenstates can be identified with the interaction eigenstates. But because of the contribution of t -channel neutralino exchange to selectron pair production, the gaugino sector of the model, mass spectrum and field contents, has to be specified to interpret the results of the searches for acoplanar electrons. With gaugino mass unification and for $\tan\beta = 1.5$ and $\mu = -200$ GeV, a selectron mass lower limit of 100 GeV is obtained for $m_{\tilde{\chi}_1^0} < 85$ GeV (88). Neutralino t -channel exchange can furthermore mediate associated $\tilde{e}_L\tilde{e}_R$ production. This process is useful if the $\tilde{e}_R - \tilde{\chi}_1^0$ mass difference is small, because the electron from the $\tilde{e}_L \rightarrow e\tilde{\chi}_1^0$ decay can be energetic enough to lead to an apparent single electron final state. Both gaugino and slepton mass unifications have to be assumed for the masses of the two selectron species to be related. Under these assumptions, a lower limit of 73 GeV was set on $m_{\tilde{e}_R}$, independent of the $\tilde{e}_R - \tilde{\chi}_1^0$ mass difference (89).

From the measurement of the invisible width of the Z boson (90), a general mass lower limit of 45 GeV can be deduced for a sneutrino LSP or NLSP.

Charginos and neutralinos: As evident from Eq. (28), three parameters are sufficient to fully specify the masses and field contents in the chargino sector.

These may be taken to be M_2 , μ , and $\tan\beta$. The lighter of the two charginos will simply be denoted “chargino” in the following. To specify the neutralino mass matrix of Eq. (26), one more parameter, M_1 , is needed. If gaugino mass unification is assumed, the two gaugino masses are related by $M_1 = (5/3) \tan^2 \theta_W M_2 \simeq 0.5M_2$. Unless otherwise specified, this relation is assumed to hold in the following. Charginos are pair produced via s -channel Z/γ^* and t -channel $\tilde{\nu}_e$ exchanges, the two processes interfering destructively. The three-body final states $f\bar{f}'\tilde{\chi}_1^0$ are reached in chargino decays via virtual W or sfermion exchange. If kinematically allowed, two-body decays such as $\tilde{\chi}^\pm \rightarrow \ell^\pm \tilde{\nu}$ are dominant. Similarly, neutralino pair or associated production proceed via s -channel Z and t -channel selectron exchanges, and $\tilde{\chi}_2^0$ three-body decays to $f\bar{f}\tilde{\chi}_1^0$ via virtual Z or sfermion exchange; whenever kinematically allowed, two-body decays such as $\tilde{\chi}_2^0 \rightarrow \nu\tilde{\nu}$ are dominant.

If sfermions are heavy, chargino decays are mediated by virtual W exchange, so that the final states arising from chargino pair production are the same as for W pairs, with additional missing energy from the two neutralino LSPs: all hadronic ($q\bar{q}'\tilde{\chi}_1^0 q\bar{q}'\tilde{\chi}_1^0$), mixed ($q\bar{q}'\tilde{\chi}_1^0 \ell\nu\tilde{\chi}_1^0$), and fully leptonic ($\ell\nu\tilde{\chi}_1^0 \ell\nu\tilde{\chi}_1^0$). Selections were designed for these three topologies and for various $m_{\tilde{\chi}^\pm} - m_{\tilde{\chi}_1^0}$ regimes, with no excess observed over SM backgrounds. From a scan over M_2 , μ , and $\tan\beta$, a chargino mass lower limit of 103 GeV was derived for $m_{\tilde{\nu}} > 200$ GeV (91). For smaller sneutrino masses, the limit is reduced by the destructive interference in the production. This limit holds for $M_2 < \simeq 1$ TeV. For larger M_2 values, the selection efficiency decreases rapidly as the $\tilde{\chi}^\pm - \tilde{\chi}_1^0$ mass difference becomes smaller. If this mass difference becomes so small that even the $\tilde{\chi}^\pm \rightarrow \pi^\pm \tilde{\chi}_1^0$ decay mode is closed, the chargino becomes long lived. Searches for charged massive stable particles, in which advantage is taken of their larger ionization power, were designed to cope with this configuration; these are described below in Sec. V.D.3. For slightly larger mass differences, the visible final state is so soft that even triggering becomes problematic. Chargino pair production can however be “tagged” by an energetic photon from initial state radiation, $e^+e^- \rightarrow \gamma\tilde{\chi}_1^+\tilde{\chi}_1^-$, providing access to those almost invisible charginos, although at a reduced effective center of mass energy. The combination of these analysis techniques allowed chargino masses smaller than 92 GeV to be excluded, irrespective of the $\tilde{\chi}^\pm - \tilde{\chi}_1^0$ mass difference (92).

For lower sfermion masses, the sensitivity of the former analyses is reduced first because of the destructive interference between the s -channel Z/γ^* and t -channel sneutrino exchanges, and second because of the opening of two-body decays. The latter effect is specifically detrimental in the “corridor” of small $\tilde{\chi}^\pm - \tilde{\nu}$ mass differences, where the final state from $\tilde{\chi}^\pm \rightarrow \ell\tilde{\nu}$ decay becomes invisible in practice. Gaugino mass unification allows indirect limits on charginos to be obtained, based on constraints on the parameter space resulting from searches for pair or

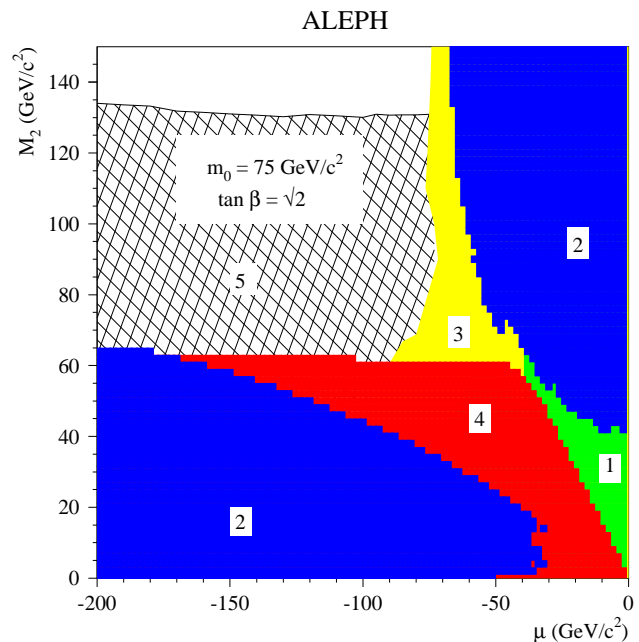


FIG. 15 Regions in the (μ, M_2) plane excluded by the LEP I constraints (1), and by the searches for charginos (2), neutralinos (3) and sleptons (4) at LEP II, for $\tan\beta = \sqrt{2}$ and $m_0 = 75$ GeV. The region (5) is excluded by the Higgs boson searches at LEP II. This figure is from Ref. (93).

associated neutralino production, e.g., $e^+e^- \rightarrow \tilde{\chi}_2^0\tilde{\chi}_2^0$ or $\tilde{\chi}_1^0\tilde{\chi}_2^0$. In order to relate all production cross sections and decay branching fractions, it is however necessary to fully specify the sfermion spectrum, which is done with the assumption of sfermion mass unification. The results of the chargino and neutralino searches are then expressed as exclusion domains in the (μ, M_2) plane for selected values of $\tan\beta$ and m_0 . The invisible two-body decay $\tilde{\chi}_2^0 \rightarrow \nu\tilde{\nu}$ can however cause a large sensitivity reduction. Since this configuration occurs for low m_0 values, constraints arising from the slepton searches can be used to mitigate this effect. With gaugino and sfermion mass unification, the slepton masses are related to the model parameters by $m_{\tilde{\ell}_R}^2 \simeq m_0^2 + 0.22M_2^2 - \sin^2\theta_W m_Z^2 \cos 2\beta$, so that a limit on $m_{\tilde{\ell}_R}$ can be turned into a limit on M_2 for given values of $\tan\beta$ and m_0 . After a proper combination of the searches for charginos, neutralinos and sleptons, an example of which is shown in Fig. 15, it turns out that the chargino mass limit obtained in the case of heavy sfermions is only moderately degraded.

Direct searches for the lightest neutralino had been performed at lower energy e^+e^- colliders, PEP and PETRA, in the reaction $e^+e^- \rightarrow \gamma\tilde{\chi}_1^0\tilde{\chi}_1^0$, where the photon from initial state radiation is used to tag the production of an invisible final state. At LEP, at or above the Z resonance, the irreducible background from $e^+e^- \rightarrow \gamma\nu\tilde{\nu}$ was too large to obtain competitive results. Furthermore, production via s -channel Z exchange may simply vanish, e.g., if the LSP is a pure photino, while production via t -channel selectron exchange can be made negligible if se-

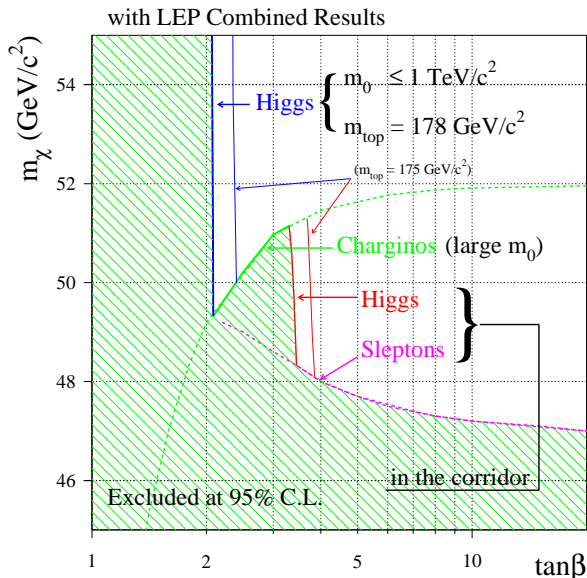


FIG. 16 Lower mass limit for the lightest neutralino as a function of $\tan\beta$, inferred in the conventional scenario from searches at LEP for charginos, sleptons, and neutral Higgs bosons (94). The dashed contour is the limit obtained for large m_0 .

lectrons are sufficiently heavy. Indirect limits on the mass of the LSP can however be obtained within constrained models. With gaugino mass unification, $m_{\tilde{\chi}_1^0}$ is typically half the chargino mass. As a result, the chargino mass limit translates into a $\tilde{\chi}_1^0$ mass lower limit of 52 GeV for heavy sfermions and large $\tan\beta$. If sfermion mass unification is used in addition, a limit of 47 GeV is obtained at large $\tan\beta$, independent of m_0 . This limit is set by searches for sleptons in the corridor. For low values of $\tan\beta$, constraints from the Higgs boson searches can be used, as was shown in Sec. III.B for benchmark scenarios. A complete scan over m_0 , $m_{1/2}$, μ and $\tan\beta$ was performed and, for each parameter set, the maximum h mass predicted was compared to the experimental limit, and the constraints from chargino and slepton searches were included. The translation of the scan result in terms of excluded domain in the $(\tan\beta, m_{\tilde{\chi}_1^0})$ plane is shown in Fig. 16, from which a $\tilde{\chi}_1^0$ mass lower limit of 47 GeV is derived (94). Within the more constrained mSUGRA scenario, wherein μ is calculated from the other parameters, this limit becomes 50 GeV (95).

Squarks: On general grounds, the mass reach for strongly interacting particles is expected to be substantially higher at the Tevatron than at LEP. For some specific configurations, however, the searches at the Tevatron become inefficient, in which cases the results obtained at LEP remain of interest. This is particularly relevant for third generation squarks which may be substantially lighter than the other squarks, as motivated in Sec. II. The lighter third generation mass eigenstates

are simply denoted stop and sbottom, \tilde{t} and \tilde{b} , in the following.

In the mass range accessible at LEP, and given the chargino mass limit which effectively forbids $\tilde{t} \rightarrow b\tilde{\chi}_1^+$, the stop is expected to decay into a charm quark and a neutralino, $\tilde{t} \rightarrow c\tilde{\chi}_1^0$, as long as $m_{\tilde{t}} < m_W + m_b + m_{\tilde{\chi}_1^0}$. Because this decay is a flavor-changing loop process, the stop lifetime can be large enough to compete with the hadronization time, and the simulation programs were adjusted to take this feature into account. The final state from stop pair production exhibits an acoplanar jet topology, for which no signal was observed above standard model backgrounds. As already explained for staus, the amount of mixing between the weak eigenstates can be such that the stop does not couple to the Z boson. In this worst case scenario, stop mass lower limits ranging from 96 to 99 GeV were obtained, depending on the $\tilde{\chi}_1^0$ mass, as long as $m_{\tilde{t}} - m_{\tilde{\chi}_1^0} - m_c > 5$ GeV (96). For smaller $\tilde{t} - \tilde{\chi}_1^0$ mass differences, long-lived R -hadrons may be produced in the stop hadronization process. The production of such R -hadrons and their interaction in the detector material were taken into account in a dedicated search, from which a stop mass lower limit of 63 GeV was derived, valid for any $m_{\tilde{t}} - m_{\tilde{\chi}_1^0}$ (97). For specific parameter choices, and in spite of the slepton mass limits, it can be that the $\tilde{t} \rightarrow b\tilde{l}\tilde{\nu}$ decay is kinematically allowed, in which case it is dominant. From a search for events exhibiting jets, leptons and missing energy, a stop mass lower limit of 96 GeV was obtained, valid for sneutrino masses smaller than 86 GeV (96).

The case of a light sbottom is much simpler, as the tree-level $\tilde{b} \rightarrow b\tilde{\chi}_1^0$ decay mode is dominant. From searches for acoplanar b -flavored jets, a mass lower limit of about 95 GeV was obtained in the worst case scenario where the sbottom does not couple to the Z (96).

2. Searches at the Tevatron

The program most widely used for the calculation of SUSY particle production cross sections at the Tevatron is PROSPINO (98), which provides next-to-leading order accuracy. The results reported below were generally obtained with the CTEQ6.1M PDF set (99). Various codes are used to calculate the low energy SUSY spectrum from initial parameters at the grand unification scale, which may introduce slight inconsistencies when comparing results in different channels or from different experiments in terms of parameters at the high scale.

Generic squarks and gluinos: Depending on the squark and gluino mass hierarchy, different pair production processes via the strong interaction are expected to contribute to $p\bar{p}$ collisions at the Tevatron: $\tilde{q}\tilde{q}$ and, to a lesser extent, $\tilde{q}\tilde{q}$, if $m_{\tilde{q}} \ll m_{\tilde{g}}$; $\tilde{g}\tilde{g}$ if $m_{\tilde{g}} \ll m_{\tilde{q}}$; and all of these processes, as well as $\tilde{q}\tilde{g}$, if the squark and gluino masses are similar. If $m_{\tilde{q}} < m_{\tilde{g}}$, the main squark decay process is expected to be $\tilde{q} \rightarrow q\tilde{\chi}_1^0$, while the main gluino decay process expected is $\tilde{g} \rightarrow \tilde{q}^*\tilde{q} \rightarrow q\tilde{q}\tilde{\chi}_1^0$ if

$m_{\tilde{g}} < m_{\tilde{q}}$. The aforementioned processes have therefore been searched for by CDF and DØ in the two-jet, four-jet and three-jet topologies, all with large \cancel{E}_T . Initial and final state radiation of soft jets can increase somewhat those jet multiplicities.

Backgrounds to squark and gluino production arise from processes with intrinsic \cancel{E}_T , such as $(W \rightarrow \ell\nu)+\text{jets}$, where the lepton escapes detection, or $(Z \rightarrow \nu\nu)+\text{jets}$, which is irreducible. Monte Carlo simulations were used to estimate those backgrounds, after calibration on events where leptons from $W \rightarrow \ell\nu$ or $Z \rightarrow \ell\ell$ are detected. Another class of background is due to multijet production by strong interaction. Although there is no intrinsic \cancel{E}_T in such events, fake \cancel{E}_T can arise from jet energy mismeasurements (and also real \cancel{E}_T from semileptonic decays of heavy flavor hadrons). In such events, the \cancel{E}_T distribution decreases quasi-exponentially, and the direction of the \cancel{E}_T tends to be close to that of a mismeasured jet. Requiring sufficiently large \cancel{E}_T and applying topological selection criteria allows this background to remain under control. While DØ applies criteria tight enough to reduce this background to a negligible level, CDF estimates its remaining contribution based on simulations calibrated on control samples.

No excesses of events were observed over SM backgrounds, which was translated into exclusion domains in the plane of squark and gluino masses. To this end, a specific SUSY model had to be specified. The reason is that the final state topology depends not only on the squark and gluino masses, but also on $m_{\tilde{\chi}_1^0}$. Moreover, additional decay modes need to be considered, such as $\tilde{q} \rightarrow \tilde{\chi}^\pm q' \rightarrow \ell\nu q' \tilde{\chi}_1^0$, which implies a full specification of the spectrum of SUSY particles. The model used by both CDF and DØ is mSUGRA, with $A_0 = 0$, $\mu < 0$, and $\tan\beta = 5$ (CDF) or 3 (DØ). The production of all squark species was considered, except for the third generation (CDF) or for stops (DØ), and the squark mass quoted is the average of the masses of the squarks considered. Finally, the large theoretical uncertainties associated to the choices of PDFs and of the factorization and renormalization scales have to be taken into account when turning cross section upper limits into exclusion domains in terms of masses. Based on an integrated luminosity of 2.1 fb^{-1} , DØ excluded the domain shown in Fig. 17, from which lower limits of 379 and 308 GeV were derived for the squark and gluino masses, respectively, as well as a lower limit of 390 GeV if $m_{\tilde{q}} = m_{\tilde{g}}$ (100). Similar results were obtained by the CDF collaboration (101).

Third generation squarks: As already mentioned, a stop NLSP decays into a charm quark and a neutralino as long as $m_{\tilde{t}} < m_W + m_b + m_{\tilde{\chi}_1^0}$. The final state from stop pair production therefore consists in acoplanar charm jets and \cancel{E}_T . Because only one squark specie is now produced, the cross section is smaller than for generic squarks, and the mass reach is therefore lower. As a consequence, the jets are softer, and there is also less \cancel{E}_T . The corresponding loss of sensitivity was attenuated by making use of heavy-flavor tagging, which resulted in the exclusion do-

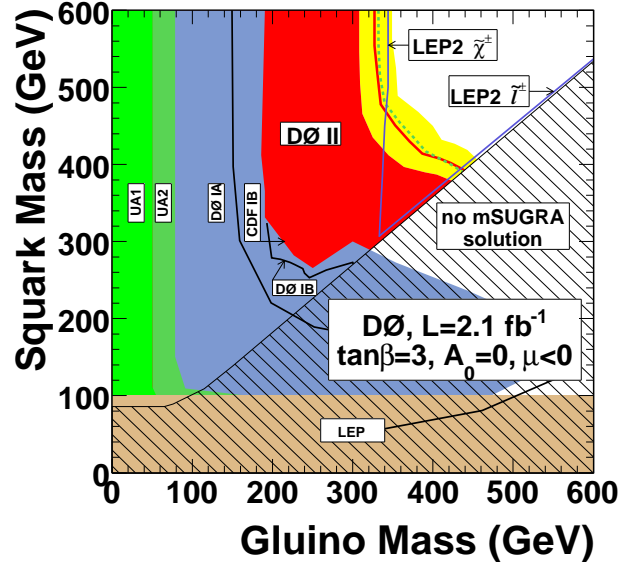


FIG. 17 Region in the $(m_{\tilde{g}}, m_{\tilde{q}})$ plane excluded by DØ (100) and by earlier experiments. The red curve corresponds to the nominal scale and PDF choices. The yellow band represents the uncertainty associated with these choices. The blue curves represent the indirect limits inferred from the LEP chargino and slepton searches.

main shown in Fig. 18, obtained by DØ (102) from an analysis of 1 fb^{-1} . It can be seen that a stop mass of 150 GeV is excluded for $m_{\tilde{\chi}_1^0} = 65 \text{ GeV}$. In spite of the larger mass reach at the Tevatron, the LEP results remain the most constraining for $\tilde{t} - \tilde{\chi}_1^0$ mass differences smaller than $\simeq 40 \text{ GeV}$. Similar searches were performed for a sbottom NLSP decaying into $b\tilde{\chi}_1^0$ (103), with better sensitivity due to a more efficient heavy-flavor tagging for b than for c quarks. A mass lower limit of 222 GeV was obtained by DØ for $m_{\tilde{\chi}_1^0} < 60 \text{ GeV}$, based on 310 pb^{-1} .

Other mass hierarchies were considered, where the stop or sbottom is not the NLSP. Three-body stop decays, $\tilde{t} \rightarrow b\ell\tilde{\nu}$, are dominant if kinematically allowed while $\tilde{t} \rightarrow \tilde{\chi}^+ b$ is not, which is possible for some model parameter choices in spite of the mass limits on charged sleptons available from LEP. The final states investigated by DØ comprised two muons or a muon and an electron, with b jets and \cancel{E}_T . Based on an analysis of 400 pb^{-1} , the largest stop mass excluded is 186 GeV, for $m_{\tilde{\nu}} = 71 \text{ GeV}$ (104). If the chargino is lighter than the stop, the $\tilde{t} \rightarrow b\tilde{\chi}^+$ decay is dominant. A search was performed by CDF in the two lepton, two b jets and \cancel{E}_T final state, with a sensitivity depending on the branching fraction of the chargino leptonic decay, $\tilde{\chi}^\pm \rightarrow \ell\nu\tilde{\chi}_1^0$, which is enhanced for light sleptons. An example of an excluded domain in the $(m_{\tilde{t}}, m_{\tilde{\chi}_1^0})$ plane is shown in Fig. 19 (105), based on 2.7 fb^{-1} . In both of those searches, the background from top quark pair production has been a major challenge. Yet another mass hierarchy was considered by CDF, namely that where the sbottom is the only squark lighter than

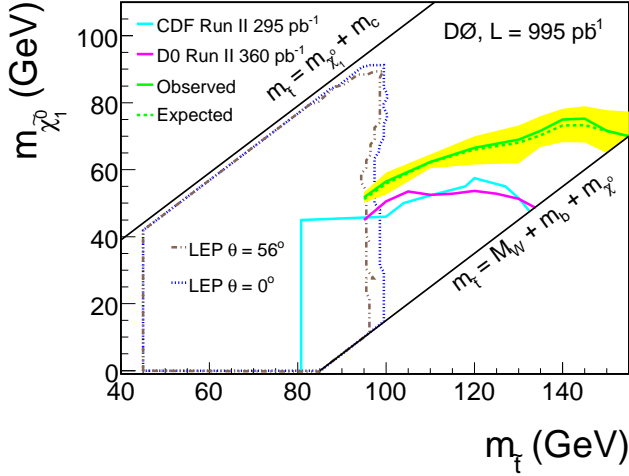


FIG. 18 Region in the $(m_{\tilde{t}}, m_{\tilde{\chi}_1^0})$ plane excluded by $D\emptyset$ (102) and by earlier experiments. The solid curve corresponds to the nominal scale and PDF choices. The yellow band represents the uncertainty associated with these choices.

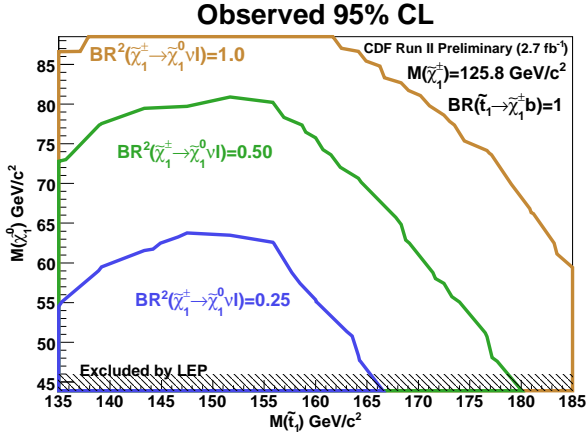


FIG. 19 Regions in the $(m_{\tilde{t}}, m_{\tilde{\chi}_1^0})$ plane excluded by CDF (105) for $m_{\tilde{\chi}_1^\pm} = 125.8$ GeV and for various values of the branching fraction for the $\tilde{\chi}_1^\pm \rightarrow \ell\nu\tilde{\chi}_1^0$ decay.

the gluino. In such a configuration, the $\tilde{g} \rightarrow b\tilde{b}$ decay is dominant, and gluino pair production then leads to a final state of four b jets and \cancel{E}_T . This search was performed in a data sample of 2.5 fb $^{-1}$, and led to excluded sbottom masses as large as 325 GeV for gluino and LSP masses of 340 and 60 GeV, respectively (106).

Charginos and neutralinos: The associated production of charginos and neutralinos, $p\bar{p} \rightarrow \tilde{\chi}_1^\pm\tilde{\chi}_2^0$, is an electroweak process mediated by s -channel W and t -channel squark exchanges. Leptonic decays, $\tilde{\chi}_1^\pm \rightarrow \ell^\pm\nu\tilde{\chi}_1^0$ and $\tilde{\chi}_2^0 \rightarrow \ell^+\ell^-\tilde{\chi}_1^0$, are mediated by W and Z exchange, respectively, and by slepton exchange. If sleptons are light, leptonic decays can be sufficiently enhanced for searches in final states consisting of three leptons and \cancel{E}_T to become sensitive in spite of production cross sections of a fraction of a picobarn. An additional challenge is the

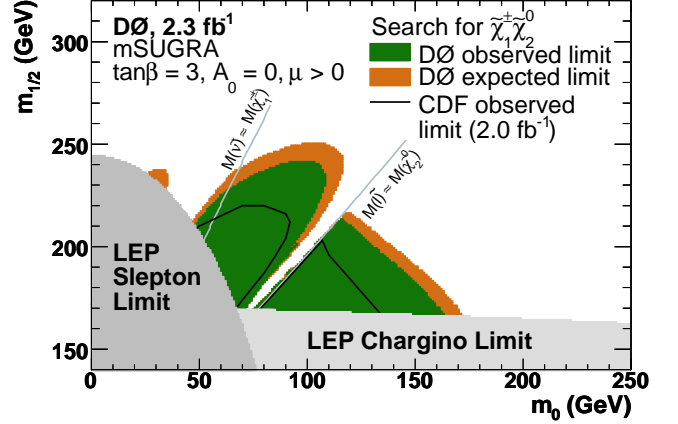


FIG. 20 Regions in the $(m_0, m_{1/2})$ plane excluded by the $D\emptyset$ search for trileptons (108).

rather small energy carried by the final state leptons in the chargino and neutralino mass domain to which the searches at the Tevatron are currently sensitive.

In both the CDF (107) and $D\emptyset$ (108) analyses, only two leptons are required to be positively identified as electrons or muons³. Allowing the third lepton to be detected as an isolated charged particle track provides sensitivity to final states including a τ lepton that decays into hadrons. In the CDF analysis, the trilepton final state is split into topologies with different signal to background ratios, the purest being when the three leptons are positively identified as electrons or muons with tight criteria. In the $D\emptyset$ approach, different selections are optimized according to the amount of energy available to the lepton candidates. The ultimate background for these trilepton searches is associated WZ production.

The $D\emptyset$ search, based on an integrated luminosity of 2.3 fb $^{-1}$, excludes regions in the mSUGRA parameter space as shown in Fig. 20 for $A_0 = 0$, $\tan\beta = 3$ and $\mu > 0$. It can be seen that the domain excluded at LEP is substantially extended by these trilepton searches. The interruption in the exclusion domain is due to configurations where the small $\tilde{\chi}_2^0 - \tilde{\ell}$ mass difference results in one of the final state leptons carrying too little energy, thus preventing efficient detection. Requiring only two leptons to be identified, but with same charge sign in order to reduce the otherwise overwhelming SM backgrounds, should provide sensitivity in that region, as was shown by $D\emptyset$ in an analysis based on a smaller data sample (109).

³ The $D\emptyset$ analysis also considers final states with a muon and one or two τ leptons identified.

D. Searches in non-canonical scenarios

1. R -parity violation

Searches for SUSY with R -parity violation were performed at LEP, the Tevatron and HERA. Both R -parity conserving pair production of SUSY particles and R -parity violating resonant single SUSY particle production were considered. The produced particles were subsequently subject to either direct or indirect (via a cascade to the LSP) R -parity violating decays. Unless otherwise specified, a single R -parity violating coupling is assumed to be non-vanishing in the following, large enough for the lifetime of the LSP to be safely assumed to be negligible.

Searches at LEP: Extensive searches for pair production were performed at LEP, involving all possible R -parity violating couplings. The possible final states are numerous, ranging from four leptons and missing energy for $\tilde{\chi}_1^0$ pair production, with decays mediated by a λ -type coupling, e.g., $\tilde{\chi}_1^0 \rightarrow e\mu\nu$, to ten hadronic jets and no missing energy for chargino pair production, with $\tilde{\chi}^\pm \rightarrow q\bar{q}'\tilde{\chi}_1^0$ followed by a $\tilde{\chi}_1^0$ decay into three quarks via a λ'' -type coupling, e.g., $\tilde{\chi}_1^0 \rightarrow udd$. The results of these searches are at least as constraining as in the canonical scenario (110).

The production of a sneutrino resonance via a λ_{1j1} coupling was also investigated. No signal was observed, and mass lower limits almost up to the center-of-mass energy were set for sufficiently large values of the R -parity violating coupling involved (111).

Searches at HERA: As explained in Sec. V.B, the HERA ep collider was most effective in the searches for R -parity violating resonant single squark production via a λ' -type coupling. Direct and indirect squark decays were investigated, and the search results were combined to lead to squark mass lower limits up to 275 GeV (112), within mild model assumptions, for a λ' coupling of 0.3, i.e., with electromagnetic strength.

Searches at the Tevatron: A fully general search for all R -parity violating couplings is not possible at the Tevatron, as it was at LEP. For instance, λ'' couplings lead to multijet final states with no or little missing energy, which cannot be distinguished from standard multijet production. Searches have therefore been designed for specific choices of couplings leading to distinct signatures.

Gaugino pair production followed by indirect decays has been extensively studied by both CDF (113) and DØ (114) in the case of a λ -type coupling. The final state is expected to contain four charged leptons, with flavors depending on the indices in the λ_{ijk} coupling, and \cancel{E}_T due to two neutrinos. For $m_0 = 1$ TeV, $\tan\beta = 5$, and $\mu > 0$, the chargino mass lower limits obtained by DØ from an analysis of 360 pb⁻¹ are 231, 229, and 166 GeV for the λ_{121} , λ_{122} , and λ_{133} couplings, respectively, with reduced sensitivity in the last case due to the occurrence of τ leptons in the final state.

Stop pair production, with $\tilde{t} \rightarrow b\tau$ via a λ'_{333} coupling

has been searched by CDF (115) in the topology where one τ decays into an electron or a muon, and the other into hadrons. From an analysis of 322 pb⁻¹, a stop mass lower limit of 151 GeV was derived.

Resonant smuon or sneutrino production could be mediated by a λ'_{211} coupling. With indirect decays, the final state would exhibit at least one muon and two jets. This topology was investigated by DØ (116), and an excluded domain was set in the $(m_{\tilde{\mu}}, \lambda'_{211})$ plane, leading to a smuon mass lower limit of 363 GeV for $\lambda'_{211} = 0.1$, and for $A_0 = 0$, $\tan\beta = 5$, and $\mu < 0$.

Resonant sneutrino production mediated by a λ'_{i11} coupling was also investigated by CDF and DØ (117), now assuming that the sneutrino decays directly via a λ -type coupling. The final states considered were ee , $e\mu$, $\mu\mu$, and $\tau\tau$. The sneutrino mass limits obtained depend on the product of the two couplings involved.

2. Gauge-mediated SUSY breaking

As already explained, the LSP in GMSB is a very light gravitino, and the phenomenology depends essentially on the nature of the NLSP, a neutralino or a stau, possibly almost mass degenerate with \tilde{e}_R and $\tilde{\mu}_R$, and on its lifetime.

Neutralino NLSP: In the mass range of current interest, a neutralino NLSP decays into a photon and a gravitino, $\tilde{\chi}_1^0 \rightarrow \gamma\tilde{G}$. Pair production of such a neutralino at LEP would therefore lead, assuming prompt decays, to a final state of two acoplanar photons and missing energy. As can be seen in Fig. 21, no excess was observed above the SM background from $e^+e^- \rightarrow (Z^{(*)} \rightarrow \nu\bar{\nu})\gamma\gamma$. In GMSB, $\tilde{\chi}_1^0$ has a large Bino component, so that pair production in e^+e^- interactions proceeds via selectron t -channel exchange. An excluded domain in the $(m_{\tilde{e}_R}, m_{\tilde{\chi}_1^0})$ plane was therefore derived (118), ruling out the GMSB interpretation (in terms of selectron pair production) of an anomalous $ee\gamma\gamma + \cancel{E}_T$ event that had been observed by CDF (119) during Run I of the Tevatron.

Searches were also performed at LEP for photons not pointing toward the interaction point, which could arise from non-prompt decays of a neutralino NLSP. For even longer lifetimes, the phenomenology becomes identical to that of the canonical scenario. The results of these various searches for a neutralino NLSP were combined with those in various topologies expected to arise from heavier SUSY particle production to lead to a robust neutralino mass lower limit of 54 GeV within the minimal GMSB framework (120).

Searches for acoplanar photons with large \cancel{E}_T were performed at the Tevatron by both CDF (121) and DØ (122). This topology is expected to arise whenever SUSY particles are pair produced, which subsequently decay to a neutralino NLSP with negligible lifetime. No excess of events was observed over the backgrounds due to photon misidentification or from fake \cancel{E}_T , all determined from data. These results were interpreted

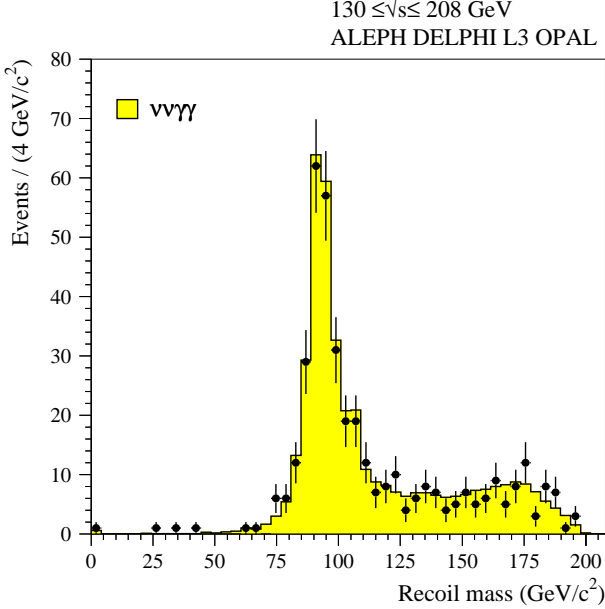


FIG. 21 Mass of the invisible system recoiling against pairs of photons at LEP (118).

within the “Snowmass slope SPS 8” benchmark GMSB model (123) where the only free parameter is the effective SUSY breaking scale Λ . The other parameters are fixed as follows: $N_5 = 1$ messenger, a messenger mass of 2Λ , $\tan\beta = 15$, and $\mu > 0$. Neutralino NLSP masses smaller than 138 GeV are excluded by the CDF analysis, based on 2 fb^{-1} .

The possibility of non-prompt neutralino NLSP decays was also investigated by CDF (124), making use of the timing information of their calorimeter. No signal of delayed photons was observed in a data sample of 570 pb^{-1} , from which an excluded domain in the plane of the mass and lifetime of the NLSP was inferred, as shown in Fig. 22 together with the result of Ref. (121).

Stau NLSP: For prompt $\tilde{\tau} \rightarrow \tau \tilde{G}$ decays, the final state arising from stau pair production at LEP is the same as in the canonical scenario with a very light $\tilde{\chi}_1^0$. For very long lifetimes, the searches for long lived charginos already reported apply. Searches for in-flight decays along charged particle tracks were designed to address intermediate lifetimes. The combination of all these searches allowed a stau NLSP mass lower limit to be set from 87 to 97 GeV, depending on the stau lifetime, as shown in Fig. 23 (125).

3. Other non-canonical scenarios

A number of searches were performed at LEP and at the Tevatron in other non-canonical scenarios.

Stable charged particles: In anomaly mediated SUSY breaking, the LSP is wino-like, and the $\tilde{\chi}^\pm - \tilde{\chi}_1^0$

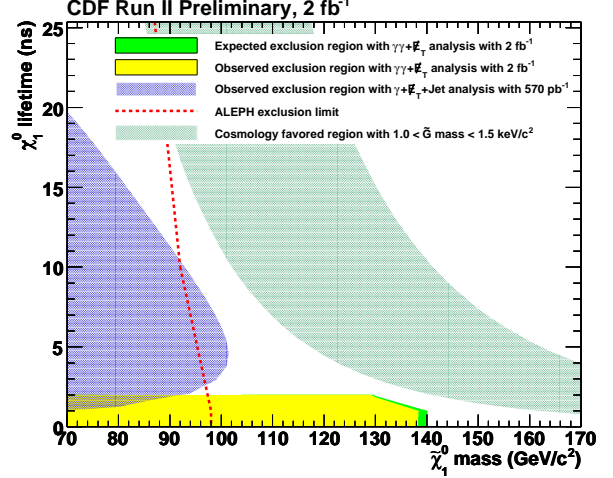


FIG. 22 Domain excluded by CDF in the plane of neutralino NLSP mass and lifetime (121; 124).

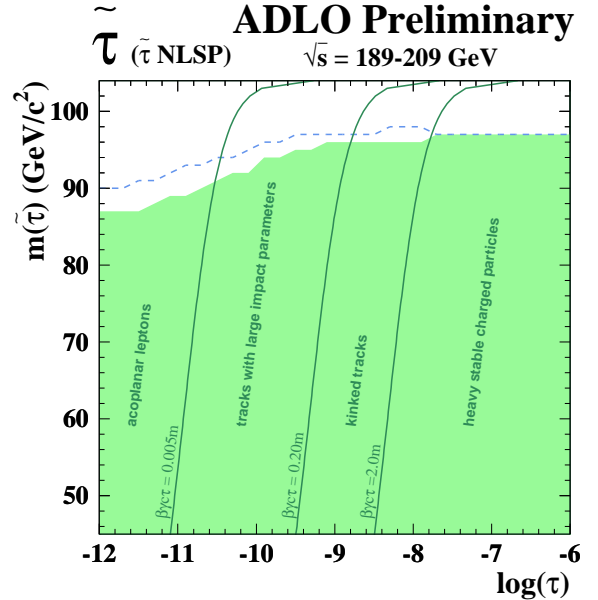


FIG. 23 Domain excluded at LEP (125) in the plane of the mass and lifetime of a stau NLSP in GMSB.

mass difference is therefore small. As a result, stable charginos are not unlikely. The searches designed at LEP in the canonical scenario for large M_2 values apply here equally well. At the Tevatron, a search was performed by $D\bar{D}$ for pairs of charged massive stable particles that could result from chargino pair production. Such particles would behave like slow moving muons that could be detected as delayed signals in the muon system. No significant excess of delayed muons was observed in 1.1 fb^{-1} , and a mass lower limit of 206 GeV was set on long-lived wino-like charginos (126).

A search for stable stops was performed by CDF in 1 fb^{-1} , using a high p_T muon trigger and their time-of-flight detector. Stable stops hadronize to form R -hadrons

which behave like slow muons. A model for the interactions of those R -hadrons with the detector material was constructed, within which a stop mass lower limit of 250 GeV was derived (127).

Stable or long-lived gluinos: Models have been built where the gluino could be the LSP and therefore stable, if R -parity is conserved (128; 129; 130). Alternatively, gluinos may decay, but with long lifetimes. This occurs, for example, in models with “split SUSY,” unnatural models in which all squarks and sleptons are very heavy, but the gauginos remain at the electroweak scale (131; 132). Since gluino decays are mediated by squark exchange, the gluino becomes long-lived.

Although gluinos cannot be produced directly in e^+e^- interactions, they could be produced via gluon splitting, e.g., $e^+e^- \rightarrow q\bar{q}g^* \rightarrow q\bar{q}\tilde{g}\tilde{g}$, and hadronize into metastable “ R -hadrons.” The QCD predictions for four-jet events would therefore be modified. Gluinos could also be produced in the decay of heavier squarks. Dedicated analyses were performed at LEP (133), leading to a mass lower limit of 27 GeV for a stable gluino.

A search for long-lived gluinos was also performed by $D\bar{O}$ with 410 pb^{-1} (134). After hadronization into an R -hadron, a long-lived gluino could come to rest in the calorimeter and decay later on, during a bunch crossing different from the one during which it was created (135). The main decay mode expected is $\tilde{g} \rightarrow g\tilde{\chi}_1^0$, leading to a hadronic shower originating from within the calorimeter and not pointing toward the $p\bar{p}$ interaction region. No excess of this anomalous topology was observed over the background due to cosmic muons or to the beam halo. The gluino mass lower limits derived depend on the lifetime $\tau_{\tilde{g}}$, the branching fraction \mathcal{B} for the decay mode considered, the $\tilde{\chi}_1^0$ mass, and the cross section σ_R for the conversion of a neutral R -hadron into a charged one in the calorimeter. As an example, a mass limit of 270 GeV was obtained for $\tau_{\tilde{g}} < 3$ hours, $\mathcal{B} = 1$, $m_{\tilde{\chi}_1^0} = 50$ GeV, and $\sigma_R = 3$ mb.

VI. SUMMARY

Supersymmetry is one of the most promising ideas for extending the standard model. When realized at the weak scale, many SUSY models provide natural, and even elegant, solutions to the most pressing problems in particle physics today by stabilizing the gauge hierarchy, providing dark matter candidates, and accommodating force unification, both with and without gravity. In addition, the general framework of weak-scale SUSY is flexible enough to encompass a wide variety of new phenomena, including extended Higgs sectors, missing energy, long-lived and metastable particles, and a host of other signatures of new physics. Searches for SUSY are therefore also searches for other forms of new physics which, even if less profoundly motivated, are, of course, also important to pursue.

In this review, we have comprehensively summarized

the state of the art in searches for SUSY at the high energy frontier. Although this a continuously evolving subject, this review provides a snapshot of the field at a particularly important time, when final results from LEP and HERA are in hand, the Tevatron experiments have reported deep probes of many supersymmetric models with several fb^{-1} of data, and the LHC will soon begin operation.

This review has summarized searches for both supersymmetric Higgs bosons and standard model superpartners. In the Higgs sector, SUSY requires a light neutral Higgs boson. This Higgs boson could be standard-model like, but it could also have non-standard couplings. In addition, it is accompanied by other Higgs bosons, both neutral or charged. The most stringent constraints on a SM-like Higgs boson currently come from LEP, with a mass lower limit of 114.4 GeV that applies in the MSSM at low $\tan\beta$. Furthermore, the LEP experiments set a lower limit of 93 GeV on the lightest neutral Higgs boson of the MSSM, independent of $\tan\beta$. The MSSM parameter space has now been further restricted by the Tevatron experiments. For example, $\tan\beta$ values larger than 40 are excluded for $m_A = 140$ GeV. For charged Higgs bosons, LEP excludes masses below 78.6 GeV, and the Tevatron experiments have extended this mass limit to ~ 150 GeV for very large values of $\tan\beta$.

For superpartners, the bounds are, of course, model-dependent, but the main results may be summarized as follows. The searches at LEP have constrained the masses of all SUSY particles, except for the gluino and the LSP, to be larger than approximately 100 GeV in most SUSY scenarios. Furthermore, an indirect lower limit on the mass of a neutralino LSP has been set at 47 GeV in the MSSM with gaugino and sfermion mass unification. The higher center-of-mass energy at the Tevatron has allowed tighter mass limits to be obtained for strongly interacting SUSY particles: 379 and 308 GeV for squarks and gluinos, respectively, within the mSUGRA framework at low $\tan\beta$. In that same model, domains beyond the LEP reach were also probed by searches for associated chargino-neutralino production.

In the near future, the first indication for SUSY at high energy colliders could be the observation of a light neutral Higgs boson at the Tevatron. Of course, such a discovery is not proof of SUSY — only the discovery of superpartners would unambiguously establish SUSY as being realized in nature. Once collisions begin at the LHC and the detectors are sufficiently understood, it will not take more than $\sim 1 \text{ fb}^{-1}$ to discover squarks and gluinos with masses less than ~ 1.5 TeV (136; 137). A new era will then begin during which the whole SUSY spectrum will have to be deciphered, and the properties of the SUSY model established. Many more fb^{-1} will be needed for that purpose, and to unravel the spectrum of SUSY Higgs bosons.

References

- [1] S. Weinberg, Phys. Rev. D **13**, 974 (1976); Phys. Rev. D **19**, 1277 (1979).
- [2] K. Wilson, unpublished.
- [3] L. Susskind, Phys. Rev. D **20**, 2619 (1979).
- [4] G. 't Hooft, in *Recent Developments in Gauge Theories*, proceedings of the NATO Advanced Summer Institute, Cargese, 1979, edited by G. 't Hooft *et al.* (Plenum, New York, 1980), p. 135.
- [5] E. Komatsu *et al.* [WMAP Collaboration], arXiv:0803.0547 [astro-ph].
- [6] Ya. B. Zeldovich, Adv. Astron. Astrophys. **3**, 241 (1965).
- [7] H.Y. Chiu, Phys. Rev. Lett. **17**, 712 (1966).
- [8] G. Steigman, Ann. Rev. Nucl. Part. Sci. **29**, 313 (1979).
- [9] R.J. Scherrer and M.S. Turner, Phys. Rev. D **33**, 1585 (1986).
- [10] H. Georgi and S. L. Glashow, Phys. Rev. Lett. **32**, 438 (1974).
- [11] S. Dimopoulos and H. Georgi, Nucl. Phys. B **193**, 150 (1981).
- [12] S. Dimopoulos, S. Raby and F. Wilczek, Phys. Rev. D **24**, 1681 (1981).
- [13] N. Sakai, Z. Phys. C **11**, 153 (1981).
- [14] L. E. Ibanez and G. G. Ross, Phys. Lett. B **105**, 439 (1981).
- [15] M. B. Einhorn and D. R. T. Jones, Nucl. Phys. B **196**, 475 (1982).
- [16] ATLAS Coll., “*ATLAS: Detector and physics performance technical design report*”, CERN-LHCC-99-14 and CERN-LHCC-99-15 (1999), “*Expected Performance of the ATLAS Experiment - Detector, Trigger and Physics*”, arXiv:0901.0512v1 [hep-ex].
- [17] CMS Coll., “*The Compact Muon Solenoid Technical Proposal*”, CERN-LHCC-94-38 (1994), “*The CMS Physics Technical Design Report*”, CERN-LHCC-2006-001 and CERN-LHCC-2006-021 (2006).
- [18] ALEPH Coll., Nucl. Instrum. and Methods **A294**, 121 (1990) and **A360**, 481 (1995).
- [19] DELPHI Coll., Nucl. Instrum. and Methods **A303**, 233 (1991) and **A378**, 57 (1996).
- [20] L3 Coll., Nucl. Instrum. and Methods **A289**, 35 (1990).
- [21] OPAL Coll., Nucl. Instrum. and Methods **A305**, 275 (1991).
- [22] H1 Coll., Nucl. Instrum. and Methods **A386**, 310 (1997) and **A386**, 348 (1997).
- [23] ZEUS Coll., “*The ZEUS Detector*”, Status Report (unpublished), DESY (1993), available on <http://www-zeus.desy.de/bluebook/bluebook.html>.
- [24] CDF Coll., Phys. Rev. **D71**, 032001 (2005).
- [25] D0 Coll., Nucl. Instrum. Methods Phys. Res. **A565**, 463 (2006).
- [26] Yu. A. Golfand and E. P. Likhtman, JETP Lett. **13**, 323 (1971) [Pisma Zh. Eksp. Teor. Fiz. **13**, 452 (1971)].
- [27] D. V. Volkov and V. P. Akulov, Phys. Lett. B **46**, 109 (1973).
- [28] J. Wess and B. Zumino, Nucl. Phys. B **70**, 39 (1974).
- [29] L. Maiani, in *Proceedings of the Summer School of Gif-sur-Yvette*, Paris (1980).
- [30] M. J. G. Veltman, Acta Phys. Polon. B **12**, 437 (1981).
- [31] E. Witten, Nucl. Phys. B **188**, 513 (1981).
- [32] H. Goldberg, Phys. Rev. Lett. **50**, 1419 (1983).
- [33] J. R. Ellis, J. S. Hagelin, D. V. Nanopoulos, K. A. Olive and M. Srednicki, Nucl. Phys. B **238**, 453 (1984).
- [34] H. Pagels and J. R. Primack, Phys. Rev. Lett. **48**, 223 (1982).
- [35] J. L. Feng, A. Rajaraman and F. Takayama, Phys. Rev. Lett. **91**, 011302 (2003) [arXiv:hep-ph/0302215].
- [36] L. Girardello and M. T. Grisaru, Nucl. Phys. B **194**, 65 (1982).
- [37] P. Fayet, Phys. Lett. B **69**, 489 (1977).
- [38] G. R. Farrar and P. Fayet, Phys. Lett. B **76**, 575 (1978).
- [39] S. P. Martin, arXiv:hep-ph/9709356.
- [40] M. E. Peskin, arXiv:hep-ph/0002041.
- [41] A. H. Chamseddine, R. L. Arnowitt and P. Nath, Phys. Rev. Lett. **49**, 970 (1982).
- [42] R. Barbieri, S. Ferrara and C. A. Savoy, Phys. Lett. B **119**, 343 (1982).
- [43] L. J. Hall, J. D. Lykken and S. Weinberg, Phys. Rev. D **27**, 2359 (1983).
- [44] L. Alvarez-Gaume, J. Polchinski and M. B. Wise, Nucl. Phys. B **221**, 495 (1983).
- [45] M. Dine, W. Fischler and M. Srednicki, Nucl. Phys. B **189**, 575 (1981).
- [46] S. Dimopoulos and S. Raby, Nucl. Phys. B **192**, 353 (1981).
- [47] C. R. Nappi and B. A. Ovrut, Phys. Lett. B **113**, 175 (1982).
- [48] L. Alvarez-Gaume, M. Claudson and M. B. Wise, Nucl. Phys. B **207**, 96 (1982).
- [49] M. Dine, A. E. Nelson and Y. Shirman, Phys. Rev. D **51**, 1362 (1995) [hep-ph/9408384].
- [50] M. Dine, A. E. Nelson, Y. Nir and Y. Shirman, Phys. Rev. D **53**, 2658 (1996) [hep-ph/9507378].
- [51] S. Dimopoulos, M. Dine, S. Raby and S. D. Thomas, Phys. Rev. Lett. **76**, 3494 (1996) [arXiv:hep-ph/9601367].
- [52] J. L. Feng and T. Moroi, Phys. Rev. D **58**, 035001 (1998) [arXiv:hep-ph/9712499].
- [53] L. Randall and R. Sundrum, Nucl. Phys. B **557**, 79 (1999) [arXiv:hep-th/9810155].
- [54] G. F. Giudice, M. A. Luty, H. Murayama and R. Rattazzi, JHEP **9812**, 027 (1998) [arXiv:hep-ph/9810442].
- [55] A. Pomarol and R. Rattazzi, JHEP **9905**, 013 (1999) [arXiv:hep-ph/9903448].
- [56] Z. Chacko, M. A. Luty, I. Maksymyk and E. Ponton, JHEP **0004**, 001 (2000) [arXiv:hep-ph/9905390].
- [57] E. Katz, Y. Shadmi and Y. Shirman, JHEP **9908**, 015 (1999) [arXiv:hep-ph/9906296].
- [58] J. L. Feng, T. Moroi, L. Randall, M. Strassler and S. f. Su, Phys. Rev. Lett. **83**, 1731 (1999) [arXiv:hep-ph/9904250].
- [59] See, e.g., R. Barbieri and M. Frigeni, Phys. Lett. **B258**, 395 (1991).
- [60] For a review of bounds on $\tan\beta$, see H. E. Haber, arXiv:hep-ph/9306207.
- [61] M. Carena, S. Heinemeyer, C.E.M. Wagner, and G. Weiglein, arXiv:hep-ph/9912223v1 and Eur. Phys. J. **C26**, 601 (2003).
- [62] ALEPH, DELPHI, L3 and OPAL Collaborations, The LEP working group for Higgs boson searches, Phys. Lett. **B565**, 61 (2003).
- [63] ALEPH, DELPHI, L3 and OPAL Collaborations, The LEP working group for Higgs boson searches, Eur. Phys. J. **C47**, 547 (2006).
- [64] The Tevatron electroweak working group for the CDF

- and DØ Collaborations, “Combination of the CDF and DØ results on the mass of the top quark”, FERMILAB-TM-2403-E (March 2008).
- [65] ALEPH, DELPHI, L3 and OPAL Collaborations, The LEP working group for Higgs boson searches, “Searches for Invisible Higgs bosons: Preliminary combined results using LEP data collected at energies up to 209 GeV”, [arXiv:hep-ex/0107032v1](#).
- [66] ALEPH, DELPHI, L3 and OPAL Collaborations, The LEP working group for Higgs boson searches, “Flavor independent search for hadronically decaying neutral Higgs bosons at LEP”, [arXiv:hep-ex/0107034v1](#).
- [67] R. Dermisek and J.F. Gunion, Phys. Rev. **D73**, 111701 (2006).
- [68] M. Carena, J.R. Ellis, A. Pilaftsis and C.E.M. Wagner, Phys. Lett. **B495**, 155 (2000) and Nucl. Phys. **B586**, 92 (2000).
- [69] The CDF Collaboration, “Search for neutral MSSM Higgs bosons decaying to tau pairs with 1.8 fb^{-1} of data”, CDF note 9071 (October 2007).
- [70] The DØ Collaboration, “Search for MSSM Higgs boson production in di-tau final states with $\mathcal{L} = 2.2 \text{ fb}^{-1}$ at the DØ detector”, DØ note 5740-CONF (July 2008).
- [71] J. Campbell *et al.*, “Higgs boson production in association with bottom quarks”, [arXiv:hep-ph/0405302v1](#).
- [72] The CDF Collaboration, “Search for Higgs bosons produced in association with b quarks”, CDF note 9284 (April 2008).
- [73] The DØ Collaboration, “Search for neutral Higgs bosons in multi-b-jet events in $p\bar{p}$ collisions at $\sqrt{s} = 1.96 \text{ TeV}$ ”, DØ note 5726-CONF (July 2008).
- [74] M. Carena, S. Mrenna and C.E.M. Wagner, Phys. Rev. **D60**, 075010 (1999) and **D62**, 055008 (2000).
- [75] The DØ Collaboration, “A search for neutral Higgs bosons at high $\tan\beta$ in the mode $\phi b \rightarrow \tau_\mu \tau_b b$ in Run IIb data”, DØ note 5727-CONF (August 2008).
- [76] DELPHI Coll., Eur. Phys. J. **C34**, 399 (2004).
- [77] OPAL Coll., “Search for Charged Higgs Bosons in e^+e^- Collisions at $\sqrt{s} = 189\text{--}209 \text{ GeV}$ ”, [arXiv:0812.0267v1 \[hep-ex\]](#).
- [78] ALEPH Coll., Phys. Lett. **B543**, 1 (2002).
- [79] L3 Coll., Phys. Lett. **B575**, 208 (2003).
- [80] ALEPH, DELPHI, L3 and OPAL Collaborations, the LEP working group for Higgs boson searches, “Search for Charged Higgs bosons: Preliminary Combined Results Using LEP data Collected at Energies up to 209 GeV”, [arXiv:hep-ex/0107031v1](#).
- [81] D0 Coll., “A search for charged Higgs bosons in $t\bar{t}$ events”, D0 Note 5715-CONF (July 2008).
- [82] J.S. Lee *et al.*, Comput. Phys. Commun. **156**, 283 (2004).
- [83] Y. Grossman, Nucl. Phys. **B426**, 355 (1994).
- [84] CDF Coll., Phys. Rev. Lett. **96**, 042003 (2006).
- [85] CDF Coll., “A search for charged Higgs in lepton+jets $t\bar{t}$ events using 2.2 fb^{-1} of CDF data”, CDF note 9322 (August 2008).
- [86] D0 Coll., “Search for charged Higgs bosons decaying to top and bottom quarks in $p\bar{p}$ collisions”, [arXiv:0807.0859v1 \[hep-ex\]](#).
- [87] V. D. Barger, G. F. Giudice and T. Han, Phys. Rev. D **40**, 2987 (1989).
- [88] LEPSUSYWG, ALEPH, DELPHI, L3 and OPAL experiments, note LEPSUSYWG/04-01.1, <http://lepsusy.web.cern.ch/lepsusy/Welcome.html>.
- [89] ALEPH Coll., Phys. Lett. **B544**, 73 (2002); L3 Coll., Phys. Lett. **B580**, 37 (2004).
- [90] The ALEPH, DELPHI, L3, OPAL, SLD Collaborations, the LEP Electroweak Working Group, the SLD Electroweak and Heavy Flavours Groups, Phys. Reports **427**, 257 (2006).
- [91] LEPSUSYWG, *ibid.*, note LEPSUSYWG/01-03.1.
- [92] LEPSUSYWG, *ibid.*, note LEPSUSYWG/02-04.1.
- [93] ALEPH Coll., Eur. Phys. J. **C11**, 193 (1999).
- [94] LEPSUSYWG, *ibid.*, note LEPSUSYWG/04-07.1.
- [95] LEPSUSYWG, *ibid.*, note LEPSUSYWG/02-06.2.
- [96] LEPSUSYWG, *ibid.*, note LEPSUSYWG/04-02.1.
- [97] ALEPH Coll., Phys. Lett. **B537**, 5 (2002).
- [98] W. Beenakker, R. Hopker, M. Spira, and P.M. Zerwas, Nucl. Phys. **B492**, 51 (1997).
- [99] J. Pumplin *et al.*, JHEP **0207**, 012 (2002); D. Stump *et al.*, JHEP **0310**, 046 (2003).
- [100] DØ Coll., Phys. Lett. **B660**, 449 (2008).
- [101] CDF Coll., “Inclusive search for squarks and gluinos in $p\bar{p}$ collisions at $\sqrt{s} = 1.96 \text{ TeV}$ ”, [arXiv:0811.2512v1 \[hep-ex\]](#).
- [102] DØ Coll., Phys. Lett. **B665**, 1 (2008).
- [103] DØ Coll., Phys. Rev. Lett. **97**, 171806 (2006); CDF Coll., Phys. Rev. **D76**, 072010 (2007).
- [104] DØ Coll., Phys. Lett. **B659**, 500 (2008).
- [105] CDF Coll., “Search for pair production of stop quarks mimicking top events signatures”, CDF note 9439 (July 2008).
- [106] CDF Coll., “Search for gluino-mediated sbottom production in the MET+b-jet sample”, CDF note 9506 (September 2008).
- [107] CDF Coll., Phys. Rev. Lett. **101**, 251801 (2008).
- [108] DØ Coll., “Search for associated production of charginos and neutralinos in the trilepton final state using 2.3 fb^{-1} of data”, [arXiv:0901.0646v1 \[hep-ex\]](#).
- [109] DØ Coll., Phys. Rev. Lett. **95**, 151805 (2005).
- [110] LEPSUSYWG, *ibid.*, note LEPSUSYWG/02-10.1; ALEPH Coll., Eur. Phys. J. **C31**, 1 (2003); DELPHI Coll., Eur. Phys. J. **C36**, 1 (2004); L3 Coll., Phys. Lett. **B524**, 65 (2002); OPAL Coll., Eur. Phys. J. **C33**, 149 (2004).
- [111] ALEPH Coll., Eur. Phys. J. **C19**, 415 (2001) and **C25**, 1 (2002); DELPHI Coll., Eur. Phys. J. **C28**, 15 (2003); L3 Coll., Phys. Lett. **B414**, 373 (1997); OPAL Coll., Eur. Phys. J. **C13**, 553 (2000).
- [112] H1 Coll., Phys. Lett. **B599**, 159 (2004); H1 Coll., Eur. Phys. J. **C36**, 425 (2004); ZEUS Coll., Eur. Phys. J. **C50**, 269 (2007).
- [113] CDF Coll., Phys. Rev. Lett. **198**, 131804 (2007).
- [114] DØ Coll., Phys. Lett. **B638**, 441 (2006).
- [115] CDF Coll., Phys. Rev. Lett. **101**, 071802 (2008).
- [116] DØ Coll., Phys. Rev. Lett. **197**, 111801 (2006).
- [117] CDF Coll., Phys. Rev. Lett. **95**, 252001 (2005); CDF Coll., Phys. Rev. Lett. **95**, 131801 (2005); CDF Coll., Phys. Rev. Lett. **96**, 211802 (2006); DØ Coll., Phys. Rev. Lett. **100**, 241803 (2008).
- [118] LEPSUSYWG, *ibid.*, note LEPSUSYWG/04-09.1.
- [119] CDF Coll., Phys. Rev. **D59**, 092002 (1999).
- [120] ALEPH Coll., Eur. Phys. J. **C25**, 339 (2002); OPAL Coll., Eur. Phys. J. **C46**, 307 (2006).
- [121] CDF Coll., “Setting Limits on GMSB Models in the $\gamma\gamma + \cancel{E}_T$ Final State at CDF”, CDF-Note 9625 (December 2008).

- [122] DØ Coll., Phys. Lett. **B659**, 856 (2008).
- [123] B.C. Allanach *et al.*, Eur. Phys. J. **C25**, 113 (2002).
- [124] CDF Coll., Phys. Rev. Lett. **99**, 121801 (2007).
- [125] LEPSUSYWG, *ibid.*, note LEPSUSYWG/02-09.2.
- [126] DØ Coll., “*Search for Charged Massive Stable Particles with the D0 detector*”, arXiv:0809.4472v1 [hep-ex].
- [127] CDF Coll., “*Search for charged, massive stable particles*”, CDF-Note 8701 (February 2007).
- [128] S. Raby, Phys. Lett. B **422**, 158 (1998) [arXiv:hep-ph/9712254].
- [129] H. Baer, K. M. Cheung and J. F. Gunion, Phys. Rev. D **59**, 075002 (1999) [arXiv:hep-ph/9806361].
- [130] S. Raby and K. Tobe, Nucl. Phys. B **539**, 3 (1999) [arXiv:hep-ph/9807281].
- [131] N. Arkani-Hamed and S. Dimopoulos, JHEP **0506**, 073 (2005) [arXiv:hep-th/0405159].
- [132] G. F. Giudice and A. Romanino, Nucl. Phys. B **699**, 65 (2004) [Erratum-*ibid.* B **706**, 65 (2005)] [arXiv:hep-ph/0406088].
- [133] ALEPH Coll., Eur. Phys. J. **C31**, 327 (2003); DELPHI Coll., Eur. Phys. J. **C26**, 505 (2003).
- [134] DØ Coll., Phys. Rev. Lett. **99**, 131801 (2007).
- [135] A. Arvanitaki, S. Dimopoulos, A. Pierce, S. Rajendran and J. G. Wacker, Phys. Rev. D **76**, 055007 (2007) [arXiv:hep-ph/0506242].
- [136] CMS Coll., J. Phys. G: Nucl. Part. Phys. **34**, 995 (2007).
- [137] ATLAS Coll., “*Expected Performance of the ATLAS Experiment - Detector, Trigger and Physics*”, arXiv:0901.0512v2 [hep-ex].